NEW ARCHAEOCETES (MAMMALIA, CETACEA) FROM THE MIDDLE EOCENE DOMANDA FORMATION OF THE SULAIMAN RANGE, PUNJAB (PAKISTAN)

BY

PHILIP D. GINGERICH, MUHAMMAD ARIF, AND WILLIAM C. CLYDE

CONTRIBUTIONS FROM THE MUSEUM OF PALEONTOLOGY

Philip D. Gingerich, Director

This series of contributions from the Museum of Paleontology is a medium for publication of papers based chiefly on collections in the Museum. When the number of pages issued is sufficient to make a volume, a title page and a table of contents will be sent to libraries on the mailing list, and to individuals on request. A list of the separate issues may also be obtained by request. Correspondence should be directed to the Museum of Paleontology, The University of Michigan, Ann Arbor, Michigan 48109-1079.

VOLS. 2-29. Parts of volumes may be obtained if available. Price lists are available upon inquiry.

NEW ARCHAEOCETES (MAMMALIA, CETACEA) FROM THE MIDDLE EOCENE DOMANDA FORMATION OF THE SULAIMAN RANGE, PUNJAB (PAKISTAN)

By

PHILIP D. GINGERICH[1], MUHAMMAD ARIF[2], AND WILLIAM C. CLYDE[1]

Abstract—Three new archaeocetes of late early Lutetian are described from the Domanda Formation of the Sulaiman Range in southwestern Punjab, Pakistan. Two are protocetids: *Takracetus simus* is distinctive in having a broad rostrum with large anterior teeth and relatively small molars; *Gaviacetus razai* is distinctive in having a very narrow rostrum. The type specimen of *G. razai* includes a *Protocetus*-like single-centrum sacrum. The third new archaeocete, *Dalanistes ahmedi*, is a large remingtonocetid preserving much of the skull, including distinctive exoccipitals. *Dalanistes*, like *Remingtonocetus*, retains a long neck, robust fused sacrum, and large hind limb. Protocetids differ from remingtonocetids in many cranial characteristics and in the postcranial skeleton, where 'caudalization' of the sacrum and reduction of the hind limb presage tail-powered swimming modifications enhanced in later archaeocetes and modern whales.

INTRODUCTION

The first mammalian remains from Eocene strata of the Sulaiman Range of Pakistan were reported by Pilgrim (1940). Pilgrim described a maxilla that he identified as anthracotheroid, and he described a partial maxilla lacking teeth and a 'bear-like' partial right pelvic bone or innominate that he identified as mesonychid creodont. These came from "blue-grey shales weathering olive-green of the lower Khirthar" at Safed Tobah, 3 to 5 miles south of Toba Kund, which is south of Kaha Nala (Fig. 1). The Khirthar stage of Indo-Pakistan was by then known to be an eastern-Tethys equivalent of the Lutetian stage of Europe, and the lower Khirthar was (and is) understood to be early middle Eocene in age. Pilgrim's (1940) report of land mammals, and the lithological descriptions of Eames (1952b,c) indicated that part of

[1]Department of Geological Sciences and Museum of Paleontology, The University of Michigan, Ann Arbor, Michigan 49109-1079, U.S.A.
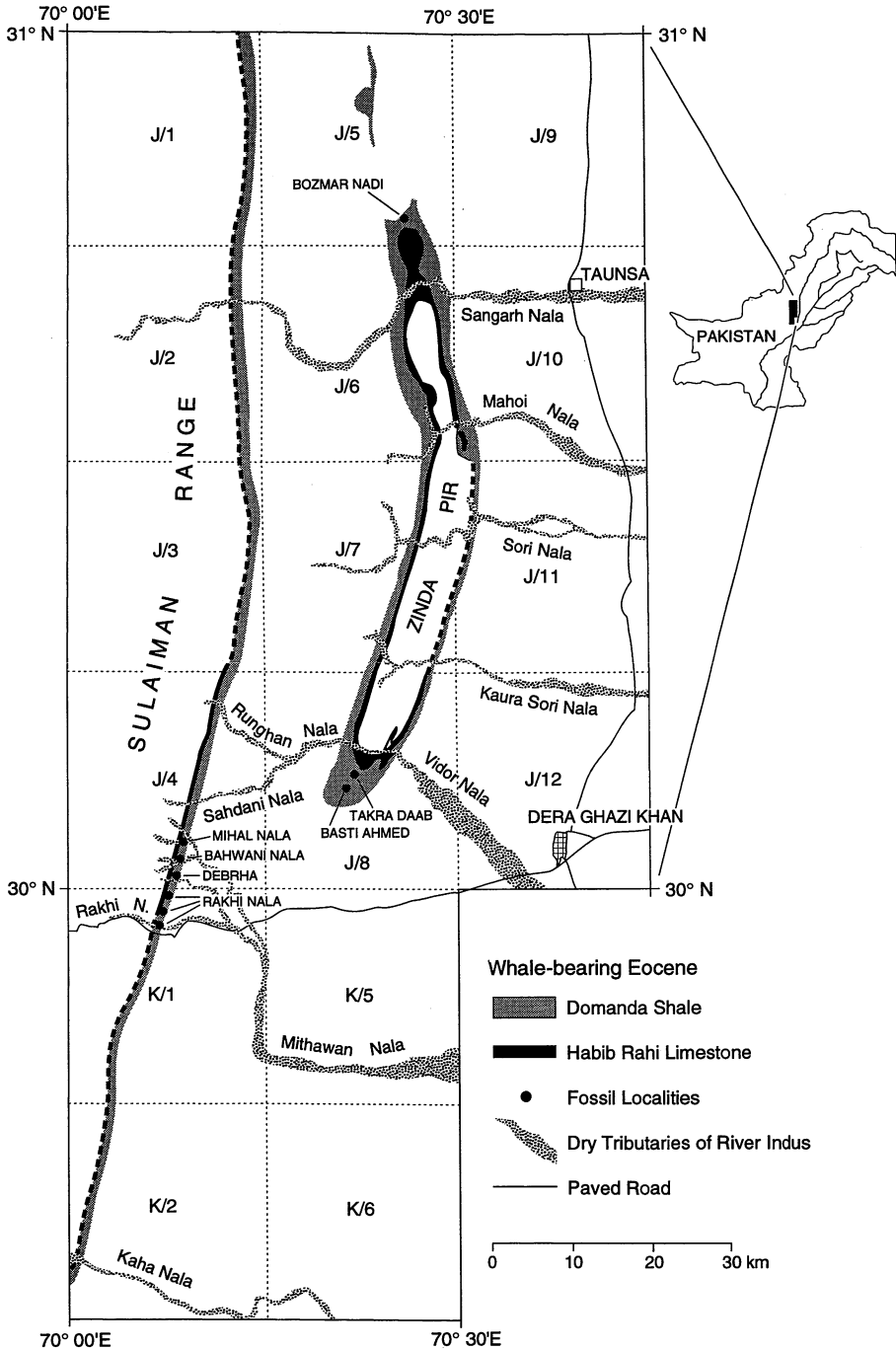[2]Geological Survey of Pakistan, 84 H-8/1, Islamabad

FIG. 1—Map of Sulaiman Range and Zinda Pir anticlinorium showing southern localities of specimens described here (Takra Daab, Basti Ahmed, Debrha, Bahwani Nala) in relation to northern localities of Bozmar Nadi specimens described by Gingerich et al. (1993, 1994).

the lower Chocolate clays, or what is now called Domanda Formation, might have been deposited in a fluvial system and yield continental mammals. A cooperative Geological Survey of Pakistan–University of Michigan [GSP-UM] research project was organized to investigate this possibility, and field work was initiated in 1977. In the field it quickly became evident that the Domanda Formation is predominantly or entirely marine.   Fragmentary cranial and postcranial remains of archaeocete cetaceans were found, and Pilgrim's edentulous 'meso-nychid' maxilla from Safed Tobah was reinterpreted as representing, possibly, an archaeocete rather than a land mammal (Gingerich et al., 1979). Pilgrim's Safed Tobah innominate and 'anthracotheroid' maxilla are also archaeocete.

During the 1970s an important new archaeocete fauna was collected and described from the marine middle Eocene of Kutch in India (Tandon, 1971, 1976; Sahni and Mishra, 1972, 1975; Satsangi and Mukhopadhyay, 1975; Trivedy and Satsangi, 1984).   Archaeocetes were also found in the marine middle Eocene of Pakistan and in what are now known to be fluvial early Eocene deposits in northern Punjab and adjacent North-West Frontier Province of Pakistan (Gingerich, 1977; West, 1980; Gingerich and Russell, 1981; Gingerich et al., 1983). All of these discoveries served to focus attention on the early and middle Eocene and eastern Tethys as the time and place of origin and diversification of Cetacea.

Exploration of the Domanda Formation continued in 1981 when a GSP-UM expedition including Neil Wells, Hassan Shaheed, David Bardack, and William Ryan found the skull included in *Indocetus* by Gingerich et al. (1993), the well preserved dentaries described as *Rodhocetus* by Gingerich et al. (1994), and a partial skull of *Remingtonocetus* cf. *R. harudiensis* described here (localities are described in Wells, 1984, and in Gingerich et al., 1993). The 1981 expedition proved that well preserved archaeocetes can be found in the Domanda Formation.

Further expeditions were organized in 1992 and 1994 to follow up on the 1981 discoveries. Field work in 1992 was concentrated at the northern plunge of the Zinda Pir anticlinorium, particularly in the Domanda Formation of Bozmar Nadi (Fig. 1). Field work in 1994 was concentrated at the southern plunge of the Zinda Pir anticlinorium, particularly in the Domanda Formation of Takra Daab (Figs. 1, 2-3). The 1994 field work yielded some 10 cetacean skulls or partial skulls, including several with good associated postcranial remains. These show, when studied together with the 1981 and 1992 collections, that there is considerable morphological and taxonomic diversity in early middle Eocene archaeocetes—much more than is seen in late middle and late Eocene archaeocetes found in Egyptian Tethys and elsewhere. Diversity and its temporal succession are important for understanding the early evolution of whales, and, while there is certainly more to discover, new associations of skulls and skeletons permit clear separation of the two principal families of early archaeocetes, Protocetidae and Remingtonocetidae, based on cranial and postcranial characteristics.

Anatomical description here follows Kellogg (1936).

ABBREVIATIONS

GSP-UM — Geological Survey of Pakistan-University of Michigan collection, Islamabad (Pakistan)

H-GSP — Howard University–Geological Survey of Pakistan collection, Islamabad (Pakistan)

LUVP — Lucknow University vertebrate paleontology collection, Lucknow (India)

NHML — Natural History Museum, London (U.K.)

VPL/K — Kumar collection, Vertebrate Paleontology Laboratory, Panjab University, Chandigarh (India)

FIG. 2—Takra valley in southern plunge of Zinda Pir anticlinorium. View is to the southeast. Exposures of soft-weathering lower Domanda Formation shales are shown in foreground, dipping to southwest and south. Center of valley in middle distance is domed erosion surface on top of Habib Rahi platy limestone. First row of hills in far distance is middle Domanda Formation dipping to southeast. Dark trees in depression on Habib Rahi surround Takra pond. Type specimen of *Takracetus sinus* came from lower Domanda shales near the left edge of the photograph.

STRATIGRAPHY

The lower Khirthar of Pilgrim (1940) or lower chocolate clays of Eames (1952b,c) are now placed in the Domanda Member of the Khirthar Formation of Hemphill and Kidwai (1973), raised to formational status by Shah (1991). The Domanda Formation is well exposed along the eastern flank of the Sulaiman Range in southwestern Punjab, where there are literally hundreds of kilometers of continuous exposure north and south of the classic Rakhi Nala section. The Domanda Formation is also well exposed in the Zinda Pir anticlinorium paralleling the Sulaiman Range, where sediments were deposited in Tethys closer to the Eocene shoreline of Indo-Pakistan (Fig. 1). We have studied the Domanda Formation intensively in three areas: (1) Rakhi Nala (see Bhatti et al., 1988); (2) Bozmar Nadi in the northern plunge of the Rodho anticline at the north end of the Zinda Pir anticlinorium; and (3) Takra Daab in the southern plunge of the Zinda Pir anticline. The Domanda Formation varies only slightly in thickness and lithology across the entire Sulaiman province.

The Domanda Formation is a 240 m thick (Takra Daab) to 300 m thick (Rakhi Nala) sequence of green and red-brown clay shales with minor limestones. There is a clear progression within the formation from green shales with limestones in the lower part of the formation; to green, brown, and red shales in the middle part of the formation; to red-brown shales at the top of the formation (Fig. 4). Siltstone is rare, and there are no courser clastics in the areas where we have studied the Domanda Formation. Invertebrate fossils are common, and typical of marine faunas found on shallow continental shelves (Eames, 1951, 1952a; Iqbal, 1969).

FIG. 3—Takra valley in southern plunge of Zinda Pir anticlinorium. View is to the south. All of the valley floor here is lower Domanda Formation shales. Type specimens of *Gaviacetus razai* and *Dalanistes ahmedi* came from middle Domanda shales in the saddle at the southwest end of the valley, southeast and south-southeast of the settlement of Basti Ahmed (approximate position of localities shown by arrows).

Takra Daab or valley (Figs. 2-3) is a tributary of Vidor Nala. The Takra Daab stratigraphic section of interest here (Fig. 4) was measured west of Takra pond, starting at the top of the underlying Habib Rahi platy limestone (poorly exposed as a broadly-domed erosion surface). At Truta, east of Takra Daab, the Domanda Formation is disturbed by faulting, and the Domanda section on the eastern side of Takra Daab may be affected by this disturbance as well. The section on the west side of Takra Daab, west of Takra pond, appears undisturbed in the lower and middle parts as high as the limestone marking the top of the middle Domanda. Part of the middle Domanda section is repeated west of Takra pond, but there is an undisturbed upper Domanda section lying above the second occurrence of the marker limestone and the repetition is easily recognized in the field (the section in Fig. 4 has the repeated part removed).

The principal Takra Daab section, including the lower and middle parts of the Domanda Formation, was measured from a point at approximately 30°08'42" N latitude and 70°21'46" E longitude (where beds strike at about 197° and dip 13°NW) to a point at 30°08'51" N and 70°21'28" E (strike 200°, dip 13°NW). After skipping the repeated part of the section, the upper Domanda Formation was measured from a point at approximately 30°09'04" N and 70°21'22" E (strike 200°, dip 17°NW) to a point at 30°09'07" N and 70°21'15" E (strike 205°, dip 16°).

The total thickness of the Domanda Formation west of Takra pond is about 240 m. The lower part of the Domanda Formation is 110 m thick, and is predominantly green shale like that separating the upper bands of platy limestone and marl in the Habib Rahi Formation. Limestone bands in the lower Domanda, eight of which form ridges and were continuous enough to trace laterally, are generally thicker (on the order of 50 cm thick) and much more widely separated vertically than are limestones of the Habib Rahi Formation. Habib Rahi limestones are off-white to tan in color, while Domanda limestone bands are generally darker brown and have a higher clastic content. The boundary between the lower and middle

Domanda is not sharp, but generally marks the transition from green shales to a 70 m thick sequence of green shales interbedded with orange, brown, and reddish-brown shales. The top of the middle Domanda is a brown, 50 cm thick limestone marker bed with oysters that weathers into very hard plates; these are resistant to weathering and tend to lag far down slope. The upper part of the Domanda Formation is about 60 m thick and it is entirely reddish-brown and brown shale, with the only variation being several conspicuous black nodular beds with oysters.

AGE OF THE DOMANDA FORMATION

The Domanda Formation was deposited on a passive continental margin on the northwestern flank of the Indo-Pakistan subcontinent before final closure of Tethys and uplift of the Himalayas. The rhythmically-bedded Habib Rahi Formation below the Domanda Formation contains closely-spaced platy limestones with brown and black cherts, alternating with green shales that thicken upward, making a smooth transition to Domanda shales as the platy limestones become thinner and finally disappear. Within the Domanda Formation there is a clear transition from green shales to green and brown shales to red-brown shales. Taken together, these lithological changes indicate a shallowing-upward cycle of marine regression from the Habib Rahi Formation through the Domanda Formation. The top of the Domanda Formation is marked by a sharp lithological change, and this is overlain by a second regressive cycle of deeper-water Pir Koh limestone shallowing upward through green and red-brown Drazinda shales. Taken together, the Habib Rahi-to-Domanda and the Pir Koh-to-Drazinda regressive cycles are very similar to each other, and their position on a passively subsiding continental margin invites interpretation in terms of global sea level sequence chronology (Haq et al., 1987).

Rhythmically-bedded Habib Rahi platy limestones with chert suggest a high-stand systems tract with deposition in deep water far enough offshore that there was little clastic input: the presence of shale interbeds may reflect climate cycles of continental weathering enhancing clastic influx. Decreasing thickness of limestone plates and increasing thickness of shale interbeds up-section reflects the beginning of relative sea level fall (seaward displacement of the shoreline). In a "type 2" sequence like that envisioned here, where subsidence is the dominant control on sediment accumulation, sediments grade progressively from high-stand to shelf-margin wedge deposits through progradation, with any subsequent cycle being initiated by flooding and renewed high-stand deposition. Transgression was too slow relative to subsidence to produce a transgressive systems tract. The Habib Rahi-to-Domanda and Pir Koh-to-Drazinda regressive cycles were evidently deposited far enough offshore, in deep enough water, that there are no major erosional hiatuses.

Stratigraphic sequences, as classified and numbered by Haq et al. (1987), are cycles of sea level transgression, which predominates in "type 1" sequences where eustatic sea level change is large relative to subsidence. Thus what we call a sea level cycle here, a regressive cycle, does not correspond to one of Haq et al.'s numbered transgressive sequences. Instead, the individual high-stand systems tracts and shelf-margin wedge or low-stand wedge tracts have to be considered individually.

Haq et al. (1987) correlated the sea level high-stand of their Tejas A sequence TA3.2 with Paleogene planktonic foraminiferal zone P10 (early Lutetian) and nannoplankton zones NP14-15; this is consistent locally with Köthe et al.'s (1988) identification of nannofossils from the Habib Rahi platy limestone of Rakhi Nala as belonging to nannoplankton zones NP14-15 (early Lutetian, ca. 47-48 Ma). Haq et al. correlated their TA3.2-TA3.3 regression with the top of P10 (early Lutetian) and NP15; this is consistent with Haq's (1972) and Köthe et al.'s (1988) identification of nannofossils from the Domanda shale of Rakhi Nala as NP15 (a relatively unconstrained early to late Lutetian). Haq et al. (1987) correlated their Tejas TA3.3 high-stand
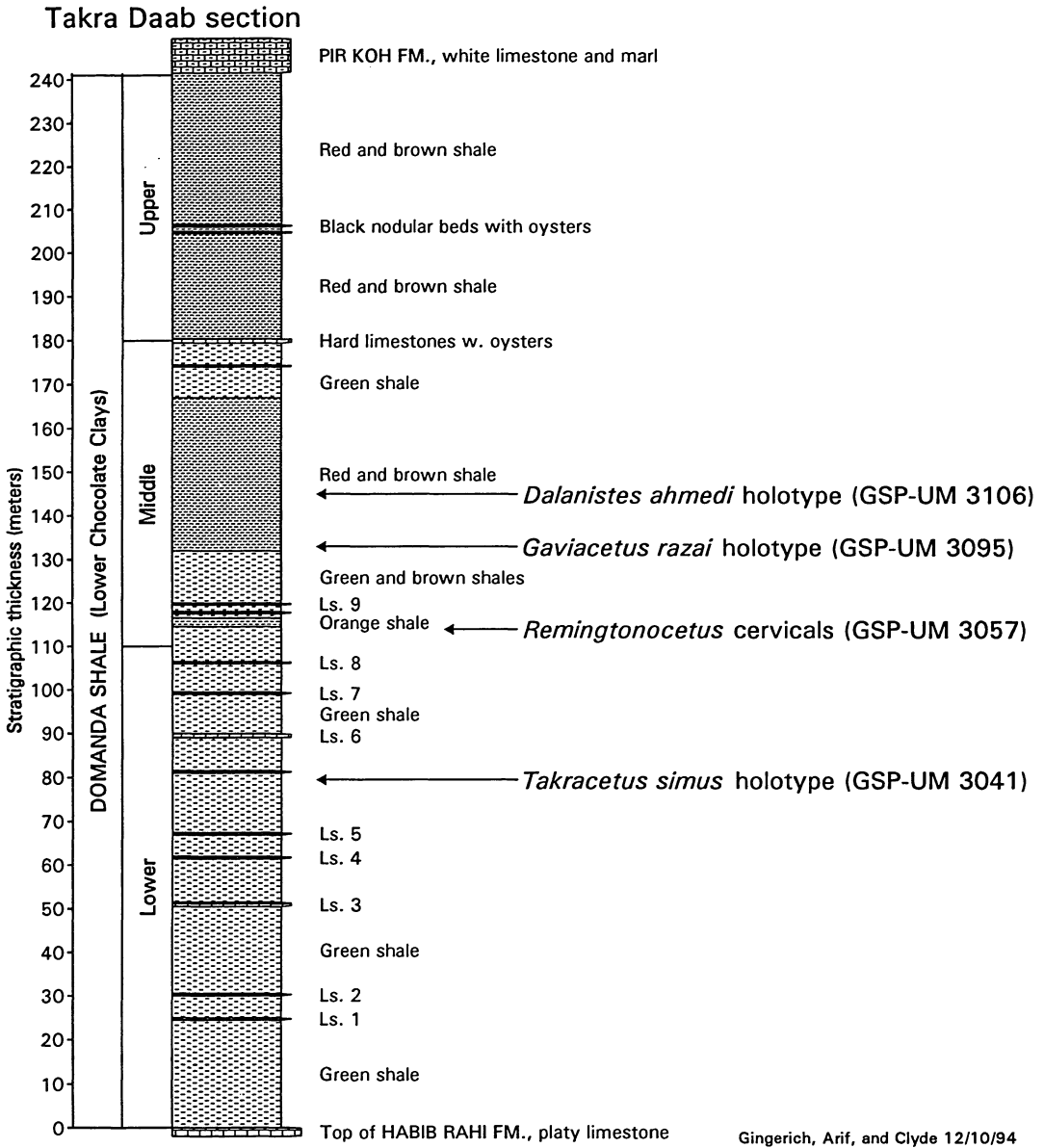
Takra Daab section

FIG. 4—Takra Daab stratigraphic section of Domanda Formation measured west of Takra pond. Arrows show stratigraphic levels yielding the principal specimens referred to in the text. Many others are known. Archaeocete specimens from Basti Ahmed were correlated with this section by tracing beds laterally. The Habib Rahi Formation below the Domanda Formation is an alternating sequence of platy limestone and green shales that thicken upward, making a smooth transition to Domanda shales as the limestones thin and disappear. The Pir Koh Formation overlying the Domanda Formation is white limestone and marl, separated from Domanda shales by a sharp lithological break. Taken together, these lithological changes indicate a shallowing-upward cycle of marine regression from the Habib Rahi Formation through the Domanda Formation, with a return to deeper-water conditions with deposition of the Pir Koh Formation. There is a clear tendency for protocetid archaeocetes to be found in the lower, deeper-water part of the section. Remingtonocetid archaeocetes predominate in the middle, shallower-water part of the Domanda Formation. The upper part of the Domanda Formation has not yet been prospected.

TABLE 1—Selected measurements of upper and lower teeth, alveoli, diastemata, cranium, and dentary of *Rodhocetus kasrani* based on GSP-UM 3012 (holotype) unless otherwise noted. Abbreviations: D, diastema following tooth; H, height; L, length; W, width. Asterisk marks estimated measurement; superscript *a* indicates estimate is of the length or width of an alveolus (alveoli in the case of teeth with multiple roots).

Cranium

		L		W		H		D	
I^1	L:W:H:D (single-rooted alveolus; GSP-UM 1853):	20.2[a]	:	12.0[a]	:	--	:	11.3	mm
I^2	L:W:H:D (single-rooted alveolus; GSP-UM 1853):	25.9[a]	:	15.3[a]	:	--	:	9.3	
I^3	L:W:H:D (single-rooted):	15.5	:	9.5	:	--	:	22.5	
C^1	L:W:H:D (single-rooted alveolus):	30.5	:	16.8	:	--	:	13.0	
P^1	L:W:H:D (single-rooted alveolus):	--	:	--	:	--	:	18.5	
P^2	L:W:H:D (double-rooted alveolus):	35.5	:	--	:	--	:	11.3	
P^3	L:W:H:D (triple-rooted alveolus):	37.5	:	14.9	:	18.8*	:	3.3	
P^4	L:W:H:D (triple-rooted alveolus):	--	:	18.0*	:	24.5*	:	--	
M^1	L:W:H:D (triple-rooted alveolus):	23.5	:	--	:	--	:	--	
M^2	L:W:H:D (triple-rooted alveolus):	24.3	:	--	:	17.8	:	--	
M^3	L:W:H (triple-rooted?):	18.2	:	16.2*	:	15.6	:	--	

Skull length (condylobasal):	61.5	cm
Diameter of orbit:	4.4*	
Diameter of infraorbital foramen:	0.64	
Breadth of frontal shield at postorbital process (maximum):	19.5	
Breadth across nasals on frontal shield (maximum):	7.6	
Breadth of rostrum at C^1:	5.8	
Breadth of rostrum at P^2:	7.0	
Breadth of palate at M^3:	14.3	
Height of skull above palate at M^{2-3}:	--	
Breadth of skull across zygomatic arches (maximum):	26.0*	
Breadth of skull across squamosals:	--	
Breadth of skull across exoccipitals:	22.0	
Foramen magnum W:H:	45.5 : 26.0	
Height of nuchal crest above foramen magnum (maximum):	10.5*	
Tympanic bulla L:W:H (width measured across sigmoid process):	6.00 : 4.60 : --	

Mandible

		L		W		H		D	
I_1	L:W:H:D (single-rooted alveolus):	--	:	--	:	--	:	--	mm
I_2	L:W:H:D (single-rooted):	21.0*	:	13.0	:	--	:	17.0	
I_3	L:W:H:D (single-rooted):	15.5	:	10.0	:	15.5*	:	15.3	
C_1	L:W:H:D (single-rooted):	32.0	:	19.0	:	36.0*	:	22.3	
P_1	L:W:H:D (incipiently double-rooted):	18.4	:	8.9	:	--	:	12.5	
P_2	L:W:H:D (double-rooted):	35.5*	:	13.4	:	--	:	9.4	
P_3	L:W:H:D (double-rooted):	42.3	:	16.2	:	34.0	:	4.5	
P_4	L:W:H:D (double-rooted):	38.6	:	14.6	:	--	:	--	
M_1	L:W:H:D (double-rooted):	23.8	:	11.9	:	--	:	--	
M_2	L:W:H:D (double-rooted):	29.0	:	15.0	:	31.6	:	--	
M_3	L:W:H:D (double-rooted):	24.5	:	13.8	:	28.7	:	--	

Length of -- dentary as preserved:	53.0	
Depth of dentary below C_1:	5.0	cm
Depth of dentary below P_{3-4}:	5.8	
Depth of dentary below M_1:	6.9	
Depth of dentary below M_3:	7.6	
Posterior opening of mandibular canal W:H:	1.60* : 6.50	

with P11 (middle Lutetian) and NP15; this is consistent with Köthe et al.'s (1988) identification of nannofossils from the Pir Koh limestone as NP15 (again relatively unconstrained early-to-late

Lutetian). Finally, Haq et al. (1987) correlated the TA3.3-TA3.4 regression with P12 (late Lutetian) and NP15-16 (middle-to-late Lutetian); this is consistent with Haq's (1972) identification of nannofossils from upper Drazinda shales as NP16 (late Lutetian). It is consistent with Samanta's (1972, 1973) identification of planktonic foraminifera from the lower Drazinda as P12-13 (late Lutetian-early Bartonian; Samanta's results must be interpreted using the Rakhi Nala section of Rieb and Bayliss published by Siddiqui, 1971). It is also consistent with Köthe et al.'s (1988) identification of nannofossils from the lower Drazinda as NP16 (late Lutetian-early Bartonian).

Taking all of the sea level and microfossil evidence together, the lower and middle Domanda Formation archaeocetes of Pilgrim, archaeocetes described by Gingerich et al. (1993, 1994), and archaeocetes described here must all come from the shelf-margin wedge at the base of sea level sequence TA3.3 at the top of planktonic foraminiferal zone P10 and within nannoplankton zone NP15. Taking planktonic foraminiferal zone P11 as middle Lutetian, Domanda archaeocetes are late early Lutetian in age (early middle Eocene) spanning a range of ca. 46 to 46.5 Ma on the Haq et al. (1987) time scale. The overlying Pir Koh high sea stand in planktonic foraminiferal zone P11 is middle Lutetian in age.

Arrows in Figure 4 show stratigraphic levels yielding the principal archaeocete specimens referred to in the following text. Archaeocete specimens from Basti Ahmed were correlated with the Takra Daab section by tracing beds laterally. There appears to be some tendency for protocetid archaeocetes to be found in the lower, deeper-water part of the Domanda Formation, while remingtonocetids predominate in the middle, shallower-water part of the Domanda Formation. No archaeocetes have been found in the upper part of the Domanda Formation, but it has not yet been thoroughly prospected.

SYSTEMATIC PALEONTOLOGY

Class MAMMALIA Linnaeus, 1758
Order CETACEA Brisson, 1762
Suborder ARCHAEOCETI Flower, 1883
Family PROTOCETIDAE Stromer 1908

Rodhocetus kasrani Gingerich et al., 1994
Fig. 6A

Indocetus ramani (in part), Gingerich et al., 1993, p. 396, figs. 2-3
Rodhocetus kasrani Gingerich et al., 1994, p. 844, figs. 1a, 3

Holotype.—GSP-UM 3012, skull with dentaries, axial skeleton from cervical vertebra C2 through caudal Ca4, ribs, left and right innominates, femur.

Type locality.—Bozmar Nadi locality 5 on map in Gingerich et al. (1995). Coordinates of locality are 30°46'06" N latitude, 70°26'37" E longitude.

Referred specimens.—GSP-UM 1852, left and right dentaries from Rakhi Nala locality RN-4. GSP-UM 1853, cranium (Fig. 6a) from Debrha.

Age and distribution.—Genus and species are known from several localities in the lower and possibly middle Domanda Formation of the Sulaiman Range and Zinda Pir anticlinorium, Pakistan, all of late early Lutetian age (middle Eocene).

Diagnosis.—*Rodhocetus* resembles later *Protocetus* and *Indocetus* cranially but differs from *Protocetus* at least in having external nares opening above C^1 and in retaining a sacrum composed of four vertebral centra.

FIG. 5—Type locality of *Takracetus simus* in the lower part of the Domanda Formation northwest of Takra Pond. Type specimen, GSP-UM 3041, was found in pieces scattered over the surface where the collector is kneeling. These were originally part of the limestone mass standing at right. The first main ridge in background is westward-dipping middle Domanda. Distant high ridges are Miocene molasse.

Description.—A preliminary description of *Rodhocetus kasrani* was published in Gingerich (1994), and a more detailed description is in preparation. Measurements of the cranium and dentaries are listed in Table 1 for comparison with those of new taxa described here.

Discussion.—*Rodhocetus* is similar to middle Lutetian *Protocetus* and late Lutetian *Indocetus*, to the extent these can be compared. All three have skulls with a rostrum of modest width. *Rodhocetus* and *Protocetus* differ in having the external nares open above C^1 and P^1, respectively, and differ in the conformation of the sacrum and pelvis (neither characteristic can be determined in specimens of *Indocetus* known to date). *Rodhocetus* was described by Gingerich et al. (1994) as having a sacrum and pelvis different from those of *Indocetus*, but the specimens called *Indocetus* in that comparison have since been reidentified from new material as *Remingtonocetus* rather than protocetid (see below). *Rodhocetus* and *Protocetus* differ in the degree of caudalization of the sacrum, and it is reasonable to expect that later *Indocetus* probably differed even more. However, this remains to be substantiated by discovery of the sacrum and pelvis of *Indocetus*.

Takracetus simus, new genus and species
Figs. 6B, 7

Holotype.—GSP-UM 3041, partial cranium.

Type locality.—West of Takra pond, on west side of Takra valley, 30°08'38" N latitude, 70°21'50" E longitude (Fig. 5).

TABLE 2—Selected measurements of upper alveoli, diastemata, and the cranium of *Takracetus simus* based on GSP-UM 3041 (holotype). Abbreviations: D, diastema following tooth; H, height; L, length; W, width. Asterisk marks estimated measurement; superscript *a* indicates estimate is of the length or width of an alveolus (alveoli in the case of teeth with multiple roots).

Cranium

I^1	L:W:H:D (single-rooted):	—	:	11.0^a	:	—	:	23.6 mm
I^2	L:W:H:D (single-rooted):	26.3^a	:	18.3^a	:	—	:	22.0
I^3	L:W:H:D (single-rooted):	16.4^a	:	15.0^a	:	—	:	48.3
C^1	L:W:H:D (single-rooted):	26.7^a	:	18.2^a	:	—	:	—
P^1	L:W:H:D:	—	:	—	:	—	:	—
P^2	L:W:H:D:	—	:	—	:	—	:	4.0
P^3	L:W:H:D (triple-rooted):	25.1^a	:	18.0^a	:	—	:	5.6
P^4	L:W:H:D (triple-rooted):	21.0^a	:	19.7^a	:	—	:	4.8
M^1	L:W:H:D (triple-rooted):	14.3^a	:	18.1^a	:	—	:	3.7
M^2	L:W:H:D (triple-rooted):	16.0^a	:	16.0^a	:	—	:	—
M^3	L:W:H (double-rooted, transverse):	8.2^a	:	12.8^a	:	—	:	—

Skull length (condylobasal):		60.0* cm
Diameter of orbit:		5.0
Diameter of infraorbital foramen W:H:	0.80 :	1.35
Breadth of frontal shield at postorbital process (maximum):		20.6
Breadth across nasals on frontal shield (maximum):		7.3
Breadth of rostrum at C^1:		9.0
Breadth of rostrum at P^2:		—
Breadth of palate at M^3:		14.3
Height of skull above palate at M^{2-3}:		7.4
Breadth of skull across zygomatic arches (maximum):		—
Breadth of skull across squamosals:		—
Breadth of skull across exoccipitals:		—
Foramen magnum W:H:	5.20 :	2.75
Height of nuchal crest above foramen magnum (maximum):		—
Tympanic bulla L:W:H (width measured across sigmoid process):	— : — :	—

Referred specimens.—GSP-UM 3070, a skull with lower jaws, cervicals, and anterior thorax from the lower Domanda Formation of Takra Daab is the right size, with large orbits and small cheek teeth, and may belong to this species (it is not yet fully prepared).

Age and distribution.—Genus and species are known only from the Takra Daab, in the lower part of the Domanda Formation, late early Lutetian (middle Eocene).

Diagnosis.—*Takracetus simus* differs from all known protocetids in having a rostrum that is broader and possibly shorter relative to other measures of cranial size, and it differs in having relatively larger orbits. Cheek teeth are smaller than those in contemporary *Rodhocetus kasrani*.

Etymology.—*Takra*, Baluch, courageous, strong; name for a tributary stream or valley in the Vidor Nala drainage, and *cetus*, L. (masc.), whale. Species name is from *simus*, L., pug-nosed, recognizing the broader rostrum of this genus and species compared to rostra of other protocetids.

Description.—The type specimen of *Takracetus simus* includes much of the cranium of a medium-sized protocetid. This is in three pieces: the anterior end of a broad rostrum; the middle part of skull with the posterior rostrum, frontal shield, orbits, and palate; and the braincase with occipital condyles but little of the basicranium. All were preserved in a fine, dense carbonate matrix that protected bone from distortion. When the skull weathered out of this matrix, pieces were scattered across a broad area of the ground. Many of these have been
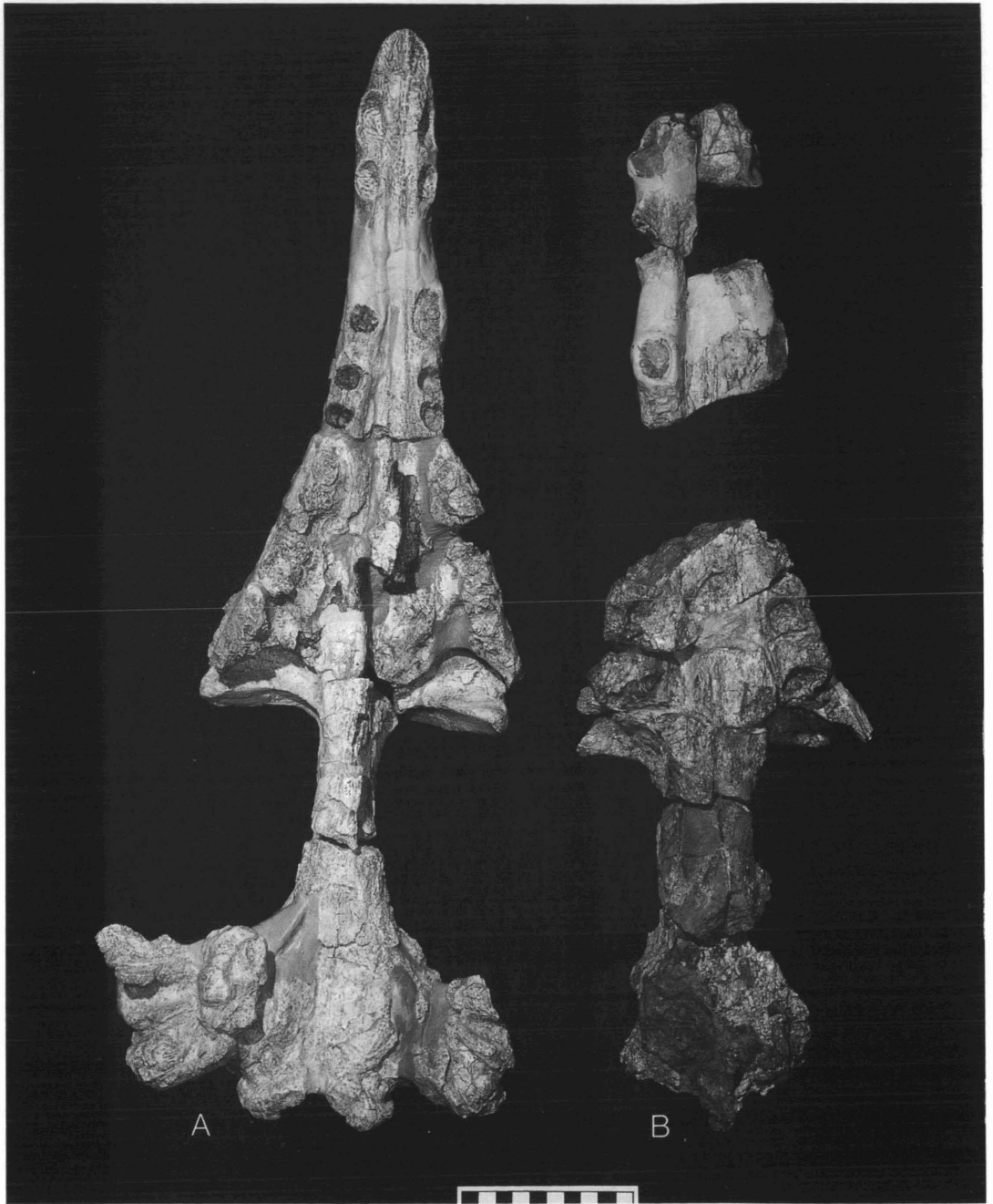
FIG. 6—Type skull of *Takracetus simus* compared to that of *Rodhocetus kasrani*. A, referred specimen of *R. kasrani*, GSP-UM 1853 (cast), in palatal view. B, type skull of *T. simus*, GSP-UM 3041, in palatal view. Note that *T. simus* is similar in size to *R. kasrani*, but the rostrum is conspicuously broader and probably a little shorter. Scale is in cm.
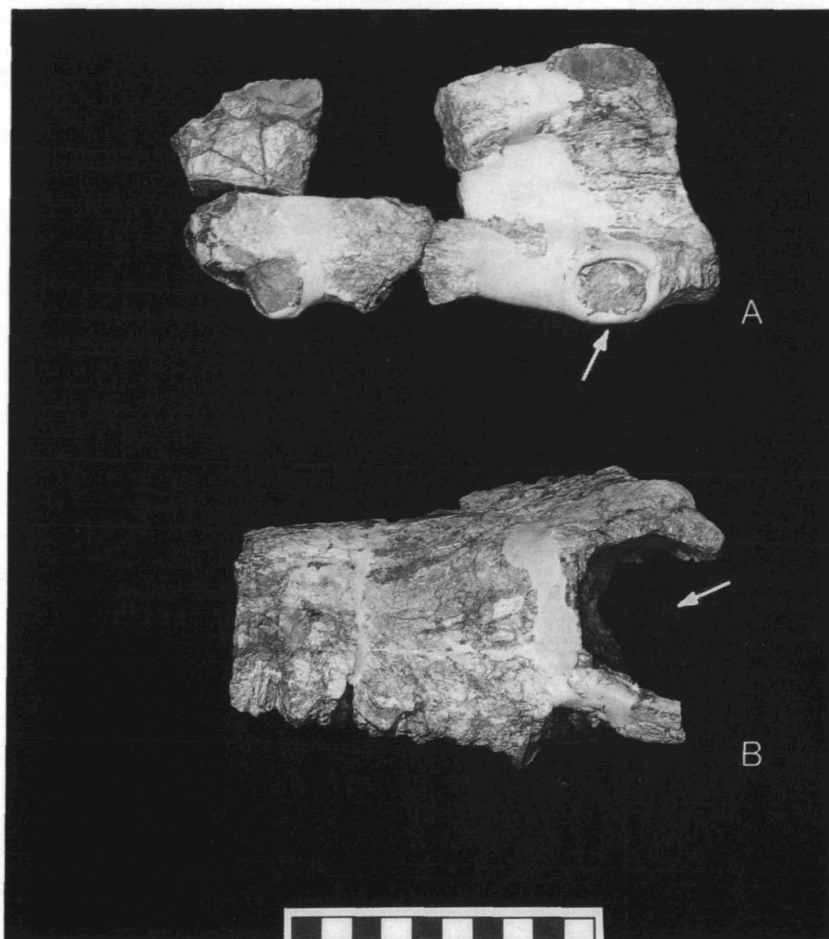
FIG. 7—Type skull of *Takracetus simus*, GSP-UM 3041. A, anterior part of rostrum in palatal view, showing alveoli for I^{1-3} and C^1 (arrow). B, middle part of skull in left lateral view; note distinctively large orbit (arrow). Scale is in cm.

reassembled to make the skull as it is now preserved, but the middle part of the rostrum with alveoli for P^{1-2} was never found. Hence the estimated condylobasal skull length of 60 cm is not well constrained.

The anterior part of the rostrum is well preserved, with roots of relatively small left and right I^1, and alveoli for relatively large I^2, small I^3, and large C^1 (measurements of alveoli are listed in Table 2). The rostrum is unusually broad for a protocetid (compare Figs. 6A and 6B), with the alveoli indicating the presence of strong teeth in life. The posterior part of the opening of the external nares is well preserved on the dorsal surface of the rostrum above the left and right alveoli for C^1.

The middle part of the cranium has the sphyroid (hammer or mallet-shaped) frontals typical of protocetids, with an intertemporal constriction between left and right temporal openings (representing the handle), and flaring supraorbital processes (representing the twin heads of the mallet). Paired nasals lap broadly over the frontals anteriorly in the middle of the skull, separating left and right maxillae from each other and separating the posterior parts of the premaxillae from the frontals. The left orbit is well preserved and this is unusually large for

TABLE 3—Selected measurements of upper alveoli, diastemata, and the cranium of *Gaviacetus razai* based on
GSP-UM 3095 (holotype). Abbreviations: D, diastema following tooth; H, height; L, length; W, width.
Asterisk marks estimated measurement; superscript *a* indicates estimate is of the length or width of an
alveolus (alveoli in the case of teeth with multiple roots).

Cranium

I^1	L:W:H:D:	--	:	--	:	--	:	--	mm
I^2	L:W:H:D:	--	:	--	:	--	:	--	
I^3	L:W:H:D:	--	:	--	:	--	:	--	
C^1	L:W:H:D:	--	:	--	:	--	:	--	
P^1	L:W:H:D:	--	:	--	:	--	:	--	
P^2	L:W:H:D (double-rooted):	26.4^a	:	10.9^a	:	--	:	23.4	
P^3	L:W:H:D (triple-rooted):	26.6^a	:	21.5^a	:	--	:	4.5	
P^4	L:W:H:D (triple-rooted):	20.0^a	:	20.8^a	:	--	:	--	
M^1	L:W:H:D:	--	:	--	:	--	:	--	
M^2	L:W:H:D:	--	:	--	:	--	:	--	
M^3	L:W:H:	--	:	--	:	--	:	--	

Skull length (condylobasal):			--	cm
Diameter of orbit:			4.8*	
Diameter of infraorbital foramen:		0.75 :	1.25	
Breadth of frontal shield at postorbital process (maximum):			20.5	
Breadth across nasals on frontal shield (maximum):			10.6	
Breadth of rostrum at C^1:			--	
Breadth of rostrum at P^2:			4.9	
Breadth of palate at M^3:			14.7*	
Height of skull above palate at M^{2-3}:			--	
Breadth of skull across zygomatic arches (maximum):			27.0*	
Breadth of skull across squamosals:			22.5	
Breadth of skull across exoccipitals:			19.5	
Foramen magnum W:H:		4.1 :	2.3	
Height of nuchal crest above foramen magnum (maximum):			10.1	
Tympanic bulla L:W:H (width measured across sigmoid process):	6.35 :	4.45 :	4.00*	

an archaeocete skull of this overall size (Fig. 7B). The palate is broad and shallowly concave
ventrally, with alveoli and roots suggesting that cheek teeth, especially upper molars, were
unusually small in comparison to anterior teeth. P^{3-4} and M^{1-2} are three-rooted, while M^3 at
the base of the zygomatic arch appears to have been transversely oriented with two roots only.
There is a shallow embrasure pit in the palate just anterolingual to the position of P^3, and deep
pits anterolingual to P^4 and M^2, but, as is typical in protocetids, there is no embrasure pit
anterolingual to M^1.

The posterior part of the skull with the braincase is not well preserved. It is essentially a
natural stone endocast of the brain with weathered bone adhering to it. The presphenoid in the
posterior part of the skull contacts the presphenoid in the middle part of the skull and stone
endocasts of narial passages contact also, permitting the two parts of the skull to be joined
(Fig. 6B). The endocast includes a long, well-developed olfactory peduncle extending forward
dorsal to the projecting presphenoid. The olfactory peduncle measures 15.8 × 8.8 mm where
it flares anteriorly beneath the frontal. Parietals are narrow anterior to the braincase and there
is a broad parietal fossa on each side anterior to the braincase for origination of deep temporalis
musculature. There is a large posterior parietal foramen visible on the left side of the top of
the braincase at the base of the nuchal crest. This foramen measures about 11 × 4 mm in
cross-section. The nuchal crest was clearly prominent in life, but this is reduced by breakage
and weathering now. The base of the left occipital condyle is preserved bordering a natural

cast of the foramen magnum at the back of the braincase.   Little is preserved of the basicranium, but the exposed endocast measures 54 mm from the midline to the left internal auditory meatus, indicating that the full endocast was about 108 mm in breadth at its maximum. Natural casts of the internal nares adhere to the ventral surface of the presphenoid and vomer.

Cranial measurements are given in Table 2.

Discussion.—*Takracetus* is clearly a protocetid archaeocete.   This is indicated by the broad and shallowly concave conformation of the palate, and the sphyroid shape of the frontals.   The broad anterior rostrum with alveoli for large anterior teeth of *Takracetus* contrasts with a palate of normal size and alveoli for relatively small posterior premolars and molars, indicating a distinctive trophic specialization not previously known in protocetids.   Large orbits may indicate that *Takracetus* was more visually-oriented than other contemporary archaeocetes (particularly remingtonocetids).

Gaviacetus razai, new genus and species
Figs. 9-11

Holotype.—GSP-UM 3095, good cranium with associated postcranial elements.

Type locality.—Basti Ahmed, in saddle to south of Takra valley, 30°07'33" N latitude, 70°21'55" E longitude (Fig. 8).

Referred specimens.—None

Age and distribution.—Genus and species are known only from the type locality in the middle part of the Domanda Formation, late early Lutetian (middle Eocene).

Diagnosis.—*Gaviacetus razai* differs from all other protocetids known in the pronounced constriction of its palate anteriorly, indicating that the rostrum was unusually narrow for a protocetid.

Etymology.—*Gavia*, L., loon, and *cetus*, L. (masc.), whale; in allusion to the narrow loon- or gavial-like rostrum of this cetacean, and the active-swimming pursuit predation suggested by the lack of fusion of sacral vertebrae.   The species is named for Dr. S. Mahmood Raza of Islamabad in appreciation of his long interest in the Eocene faunas of Pakistan and his many contributions to collaboration in field work.

Description.—The cranium of the type was found weathering from a sulphurous clay shale. It is slightly compressed dorsoventrally and all of the teeth are missing. There are no roots in the alveoli, and it appears that the teeth fell out of the skull before burial. The rostrum anterior to P^2 was missing when the specimen was found, and it too may have been lost before burial.

The dorsal surface of the middle part of the cranium is dominated by unusually broad nasals that lap high up onto the frontal shield. The frontals are sphyroid, with a narrow tongue of bone inserting between left and right nasals, and broad supraorbital processes. The frontals interdigitate with parietals in the intertemporal constriction. Left and right frontal bones are knit together with a suture of great complexity.

The intertemporal constriction is broken in a way that shows the course of the olfactory peduncle, represented by a natural stone cast coming forward from the brain and rising at an angle of a few degrees relative to the occlusal plane of the maxillary teeth. The olfactory peduncle measures about 14 mm in diameter at its narrowest, and 21.8 × 11.6 mm where it begins to flare anteriorly. Casts of the optic nerves lie just ventrolateral to the olfactory pedicle; these appear to be about 4-5 mm in diameter. Finally, natural casts of the opthalmic and maxillary branches of the trigeminal nerve form a single mass on the left and right sides, lateral to the optic nerves. These trigeminal branches are about 12 mm in diameter and run parallel to the olfactory peduncle before emerging through the orbital fissure and dividing. The course of the opthalmic nerve is not clear, but its main branch, the maxillary nerve, turns laterally and must have descended to enter the pterygopalatine fossa, sphenopalatine fissure, and then maxillary canal, finally emerging from the infraorbital foramen. All three of these
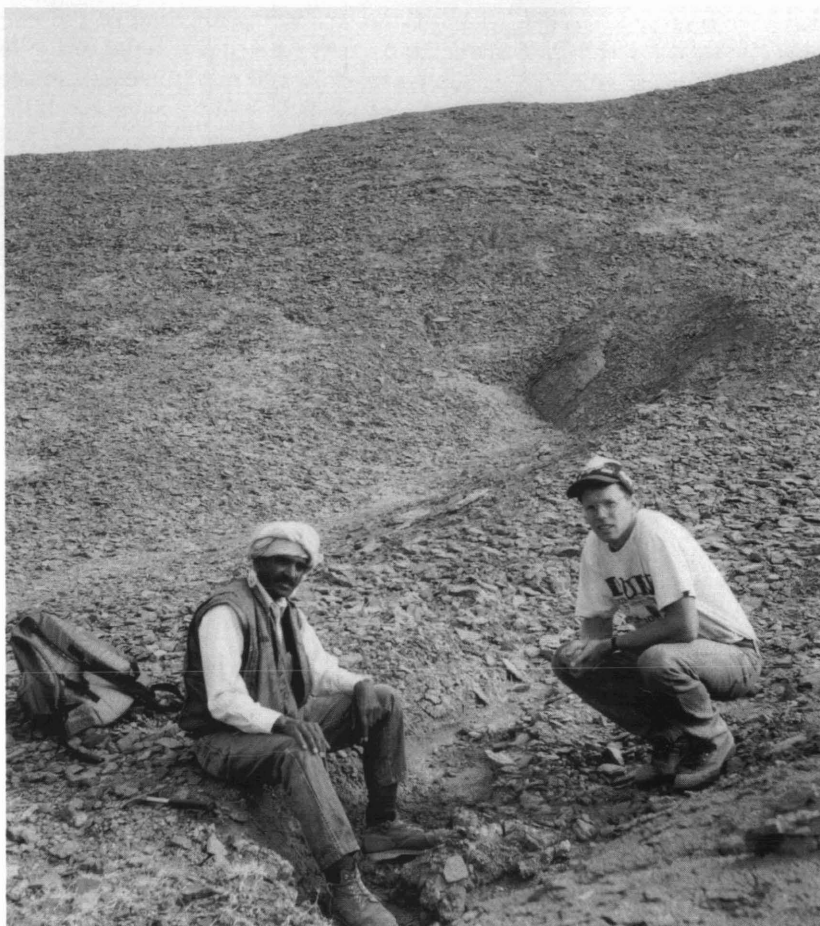
FIG. 8—Type locality of *Gaviacetus razai* in middle Domanda Formation shales southeast of Basti Ahmed
in the saddle shown in Figure 3. Type specimen was found between two collectors, where it was
exposed in situ by erosion. Sacral and proximal caudal vertebrae were found with rib fragments
within a meter of the skull. View here is to the northeast.

important nerves, olfactory, optic, and trigeminal, lie in channels on top of the presphenoid.
The orbits themselves face laterally and slightly forward. They are large, but a little smaller
than those of *Takracetus*.

The palate is markedly concave ventrally, with alveoli for the posterior cheek teeth
projecting well below the middle part of the palate. Alveoli for a double-rooted P^2 and triple-
rooted P^3 are well preserved. Alveoli on the right side of the palate show P^4 to have been
triple-rooted. There is no alveolus for a medial root of P^4 on the left side, suggesting that the
tooth may have been broken and the alveolus resorbed while the animal was alive. Alveoli for
M^1 on the right side show this tooth to have had a medial root, although these and all other
upper molar alveoli are missing due either to damage in life or postmortem breakage. The
roots of both zygomatic arches are broken and missing, and these undoubtedly carried alveoli
for M^3 (assuming M^3 was present as it is in other protocetids).

Palatine bones are wedged between maxillae as far forward as P^4 in the palate. Posteriorly
the palatines have prominent ridges for muscle attachment that converge in the midline where

they are sutured to pterygoids. Together they form the ventral surface of the paired narial passages. These passages, now filled by sedimentary matrix, are separated medially and dorsally by thin laminae of the vomer, with the dorsal laminae replaced posteriorly by laminae of the pterygoids (where exactly this happens is not clear). The posterior edges of dorsal laminae of the pterygoids are visible as a thin transverse edge of bone where these extend posteriorly onto the basioccipital, covering the basisphenoid and the basisphenoid-basioccipital suture completely. The posterior surface of the pterygoids is broken ventrally and it is not clear exactly where the internal narial opening was positioned. Narial passages appear to have been covered ventrally to within 3-4 cm in front of the auditory bullae.

The tympanic (ectotympanic) auditory bulla is well preserved on the right side of the skull. It appears to be dense like those of other early archaeocetes. The long axis of the bulla is directed anteroposteriorly, and the long axis of the bulla is almost parallel to the long axis of the skull. The lateral surface of the bulla is flat and nearly circular, with the plane of the surface being very nearly parasagittal. A prominent sigmoid process develops from the anterior edge of the circular lateral surface. These and their medial involution taken together are part of the lateral lobe of the bulla. A narrow sulcus separates the flat lateral surface of the lateral lobe from an ovally-involuted anterior lobe, and a broader shallow sulcus separates both from an ovally-involuted posterior lobe. Comparison of the right side of the skull, where the bulla is present, with the left side where it is absent, shows that the tympanic bulla has three substantial contacts with the rest of the cranium: (1) the anterior lobe has a dorsal synchondrosis with a broad, flat, circular surface of the squamosal (clearly seen on the left side of the skull where the bulla is missing); (2) the posterior process of the lateral lobe has a dorsal synostosis with the posterior process of the periotic (this contact is broken on the left side of the skull); and (3) the posterodorsal corner of the posterior lobe contacts a narrow paroccipital process of the exoccipital in another synchondrosis. There are two additional contacts or near contacts: (4) the sigmoid process of the lateral lobe fills a space medial to the postglenoid process of the squamosal; and (5) the medial surface of the posterior lobe of the bulla lies close to the falcate or lateral process of the basioccipital-exoccipital just anterior to the jugular notch.

The periotic or petrosal is exposed on the left side of the cranium, but surface detail is not well preserved. The periotic merges indistinguishably with the squamosal anteriorly, and the posterior process of the periotic is sandwiched between squamosal and exoccipital posterolaterally. There is no indication of any development of a pterygoid sinus between the pterygoid and squamosal anterior to the periotic. Falcate processes of the basioccipital-exoccipital are not divided as they are in later archaeocetes.

Other features of the posterior part of the cranium worthy of note are a relatively low sagittal crest sweeping upward posteriorly to join a high semicircular nuchal crest. There is a large posterior parietal foramen on each side of the top of the braincase at the base of the nuchal crest. Occipital condyles are large, narrow, and obliquely oriented. There is a pair of weakly developed mamelons on the supraoccipital just above the foramen magnum. Exoccipitals flare laterally and ventrally from the occipital condyles. These are rectangular, measuring some 57 mm deep from dorsal to ventral edges. The posterior surfaces of the exoccipitals are relatively flat, and there are no prominent ventrolateral processes like those seen in remingtonocetids (see below). Measurements of the cranium are given in Table 3.

The only postcranial remains of *Gaviacetus* are a rib and two vertebrae found with the type specimen (Fig. 11). The rib appears to be from the middle of the thorax and is notable only in being more gracile than those associated with the type of *Rodhocetus kasrani*. It measures about 14.8 × 9.0 mm in cross-section just below the tuberculum.

One of the vertebrae is a reasonably complete first sacral (S1; Fig. 11B). This is distinctive in lacking fusion to a second sacral centrum, in having smooth laminae of the neural arch with no evidence of articular contact with laminae of S2 (as there is in *Rodhocetus kasrani*), and in having a robust, flaring, transverse process on the right side. There does not appear to be any pleurapophyseal articulation between this transverse process and any on S2 (as there is in

FIG. 9—Type skull of *Gaviacetus razai*, GSP-UM 3095, in A, dorsal, and B, ventral views. Sphyroid shape of frontals and conformation of exoccipitals and bulla indicate that *Gaviacetus* is a protocetid, but narrowing of the palate anterior to P^2 (arrows) is different from that seen in any other protocetid known. Scale is in cm.

R. kasrani). The lateral surface of the transverse process is angled, flaring anteriorly like the auricular surface in *Rodhocetus*, and it appears likely that there was a real auricular surface for articulation with the ilium although the broader edges that would confirm this are broken. The centrum of S1 measures 46.0 × 51.8 × 38.7 mm in length, width, and height, respectively. The neural canal is kidney-shaped and measures 32.4 × 13.5 mm in cross section. The transverse process on the right side extends 59 mm laterally from the midline of the centrum, meaning that the whole sacrum was about 118 mm wide when left and right transverse processes were both present. The sacrum of *Gaviacetus* is very similar to that of *Protocetus* illustrated by Fraas (1904, pl. 3, figs. 8-9; Stromer, 1908, corrected Fraas' erroneous reconstruction of this as having two neural spines), but the transverse processes of S1 in *Gaviacetus* are much more robust.

The second vertebra is an anterior caudal similar to Ca1 in *Rodhocetus*. It does not articulate well with S1, and hence must be one or more vertebrae posterior to S1 in the verte-
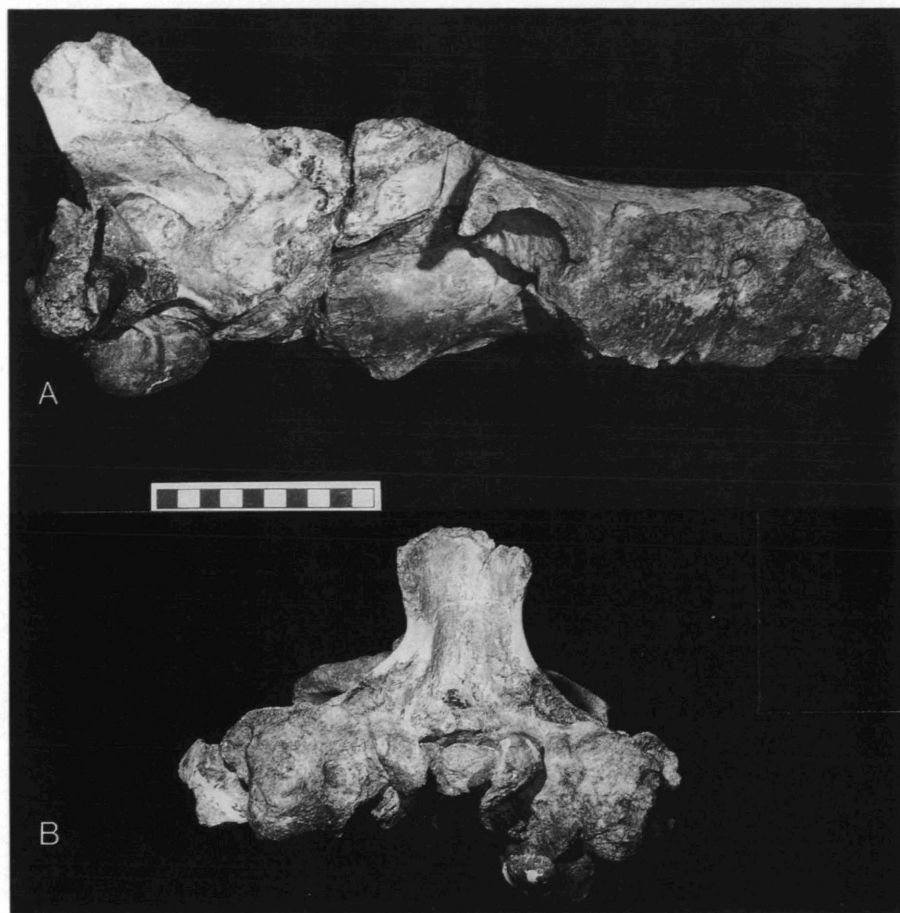
FIG. 10—Type skull of *Gaviacetus razai*, GSP-UM 3095, in A, lateral, and B, posterior views. Conformation of exoccipitals and bulla and relatively large orbit indicate that *Gaviacetus* is a protocetid. Scale is in cm.

bral column. The centrum measures $44.0 \times 52.0 \times 36.3$ mm, and the triangular neural canal measures 27.5×16.5 mm.

Discussion.—*Gaviacetus* has a very narrow rostrum anterior to P^3, while the rest of the skull is typically protocetid. This indicates a distinctive trophic specialization, but it is difficult to determine what this might be without having any of the teeth preserved and without knowing the total length of the rostrum.

The sacrum in *Gaviacetus*, with a single-centrum and robust transverse processes, is intermediate in form between those of *Rodhocetus* and *Protocetus*. Discovery that *Gaviacetus* had a sacrum with no fusion to S2 (if there was even a second vertebra in the sacrum) indicates caudalization of the vertebral column beyond that seen in *Rodhocetus* and suggests that *Gaviacetus* was probably a better tail-powered swimmer comparable in grade to *Protocetus*.

The narrow rostrum of the skull and the caudalized sacrum of *Gaviacetus* make it reasonable to infer that *Gaviacetus* was a pursuit predator like other protocetids for which we have adequate representation of the postcranial skeleton.
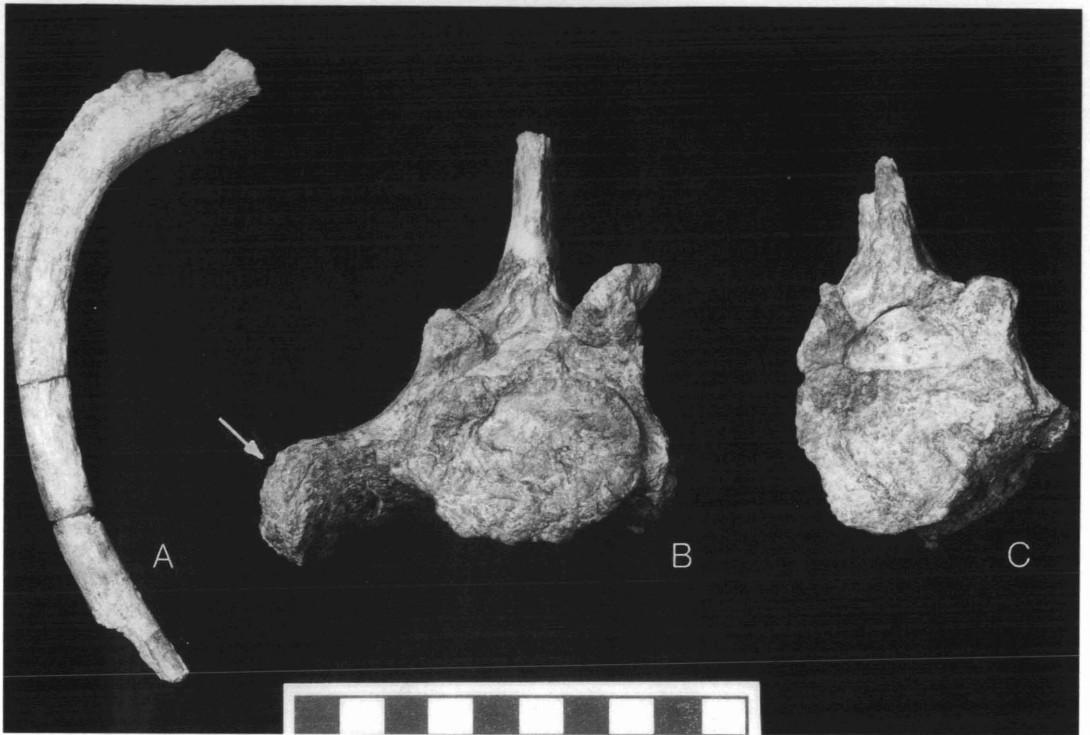
FIG. 11—Postcranial remains associated with the type skull of *Gaviacetus razai*, GSP-UM 3095. A, nearly complete mid-thoracic rib. B, sacral vertebra S1, in anterior view. C, anterior caudal vertebra, possibly Ca3, in anterior view. Note robust transverse process, expanding distally, on right side of sacrum (arrow; this is broken on left side [right side of photograph]). The broader distal edges of the transverse process here are broken, but the distal surface diverges from the midline anteriorly and it appears likely that there was a real auricular surface and a real synchondrosis with the ilium, as there probably was in *Protocetus* with similar angulation. The centrum of S1 was not fused to more-posterior sacral centra, suggesting that *Gaviacetus* was probably a tail-powered swimmer like *Protocetus* and *Rodhocetus*. Scale is in cm.

Family REMINGTONOCETIDAE Kumar and Sahni, 1986

Remingtonocetus cf. *R. harudiensis* (Sahni and Mishra, 1975)
Figs. 12-15

Protocetus harudiensis Sahni and Mishra, 1975, p. 21, Pl. 4: 4-7
Protosiren fraasi (in part), Sahni and Mishra, 1975, p. 27, fig. 4, Pl. 6: 1
Cf. Moeritheriid sacrum, Sahni and Mishra, 1975, p. 29, fig. 5, Pl. 6: 2
Remingtonocetus harudiensis, Kumar and Sahni, 1986, p. 330, figs. 3-10
Indocetus ramani (in part), Gingerich et al., 1993, p. 399, figs. 4-8, 9A,B, 10A, 12B, 13A-C

Holotype.—LUVP 11037, fragmentary skull with roots for P^4-M^3, isolated cusps of upper teeth, left mandibular ramus with roots for P_4-M_3, crowns of left M_1 and M_2, and right mandibular fragment with roots for P_4-M_2.
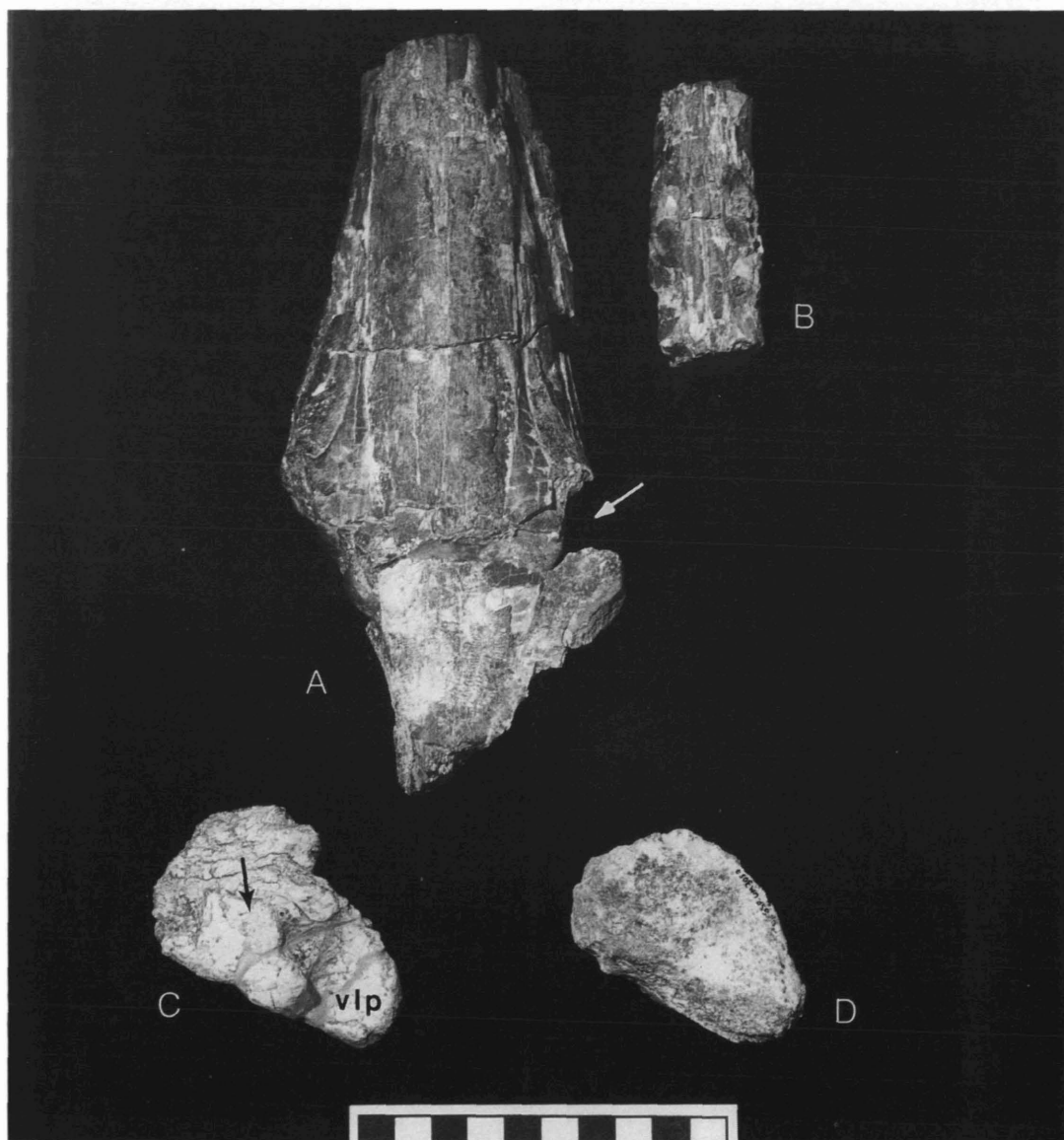
FIG. 12—Cranial remains of *Remingtonocetus* cf. *R. harudiensis*. A, middle part of skull, GSP-UM 1856, in dorsal view; note small opening for orbit (arrow). B, rostrum fragment of GSP-UM 1856, in palatal view. C, left exoccipital of GSP-UM 3009 (cast) in anterior view; note ventrolateral process (*vlp*) extending beyond paroccipital surface for articulation with bulla (arrow). D, right exoccipital of GSP-UM 3057 in posterior view. Scale is in cm.

Type locality.—Chocolate Limestone, Babia Stage (Berwali Series), 2 km north of Harudi, southwestern Kutch, Gujarat, India (23°30'20" N latitude, 68°41'15" E longitude).
. *Referred specimens from Pakistan.*—1981 collection: GSP-UM 1856, partial skull with associated piece of rostrum (Fig. 12A,B). 1992 collection: GSP-UM 3009, cranial fragments (presphenoid, exoccipital–Fig. 12C), vertebrae, sacrum, acetabulum of pelvis; and GSP-UM 3015, cranial fragments (presphenoid), vertebrae, proximal femur, tibia (described by

TABLE 4—Selected measurements of upper alveoli, diastemata, and the cranium of *Remingtonocetus* cf. *R. harudiensis* based on GSP-UM 1856. Abbreviations: D, diastema following tooth; H, height; L, length; W, width. Asterisk marks estimated measurement; superscript *a* indicates estimate is of the length or width of an alveolus (alveoli in the case of teeth with multiple roots).

Cranium

		L		W		H		D	
I^1	L:W:H:D:	--	:	--	:	--	:	--	mm
I^2	L:W:H:D:	--	:	--	:	--	:	--	
I^3	L:W:H:D:	--	:	--	:	--	:	--	
C^1	L:W:H:D (single-rooted, deciduous?):	8.7*	:	8.6*	:	--	:	--	
P^1	L:W:H:D (single-rooted, deciduous?):	9.2*	:	7.2*	:	--	:	--	
P^2	L:W:H:D:	--	:	--	:	--	:	--	
P^3	L:W:H:D:	--	:	--	:	--	:	--	
P^4	L:W:H:D:	--	:	--	:	--	:	--	
M^1	L:W:H:D (triple-rooted):	29.0*	:	15.0*	:	--	:	--	
M^2	L:W:H:D:	--	:	--	:	--	:	--	
M^3	L:W:H (double-rooted):	--	:	--	:	--	:		

Skull length (condylobasal):		--	cm
Diameter of orbit:		--	
Diameter of infraorbital foramen:		--	
Breadth of frontal shield at postorbital process (maximum):		10.7*	
Breadth across nasals on frontal shield (maximum):		4.15*	
Breadth of rostrum at C^1:		2.8	
Breadth of rostrum at P^2:		7.2	
Breadth of palate at M^3:		9.8	
Height of skull above palate at M^{2-3}:		7.8	
Breadth of skull across zygomatic arches (maximum):		--	
Breadth of skull across squamosals:		--	
Breadth of skull across exoccipitals:		--	
Foramen magnum W:H:	--	:	--	
Height of nuchal crest above foramen magnum (maximum):		--	
Tympanic bulla L:W:H (width measured across sigmoid process):	-- : -- : --		

Gingerich et al., 1993, and erroneously identified as *Indocetus ramani*). 1994 collection: GSP-UM 3054, much of left femur and proximal epiphysis of tibia (Fig. 15); 3057, cranial fragment (exoccipital–Figs. 12D, 13K), vertebrae including a good cervical and anterior thoracic series (Figs. 13A-J, 14), with rib and other fragments; and 3101, fragmentary part of middle of skull including frontal sinus and part of orbit.

Age and distribution.—Genus and species are known from several localities in India and Pakistan. In Pakistan the species is known principally from the middle part of the Domanda Formation at the southern end of the Zinda Pir anticlinorium and from Rakhi Nala in the Sulaiman Range, Punjab, Pakistan. The record from Kohat District, Pakistan, reported in Kumar and Sahni (1986, p. 331) is based on a misunderstanding: the specimen in question, GSP-UM 1856, is from Bahwani Nala in the Sulaiman Range of southwestern Punjab. These are all late early Lutetian (middle Eocene) in age.

Diagnosis.—See Kumar and Sahni (1986, p. 330) for diagnosis and a thorough description of better specimens than those available here.

Description.—New cranial specimens add little to the extensive description of good specimens published by Kumar and Sahni (1986). GSP-UM 1856 is a partial skull in two pieces. The middle part of the skull is virtually identical in comparable parts to VPL/K 15002, a paratype of *Remingtonocetus harudiensis* illustrated by Kumar and Sahni (1986, fig. 10B,C). GSP-UM 1856 shows the relatively narrow rostrum, domed dorsally in a semicircular cross-

TABLE 5—Sizes of vertebrae of *Remingtonocetus* cf. *R. harudiensis*, based on GSP-UM 3057 (Fig. 14). Axis length in parentheses is functional length. Width in parentheses is measured over rib facets. Superscript *h* means hypophysis is included. Asterisk marks estimates. Measurements are in mm.

Vertebra	Centrum			Neural canal	
	Length	Width	Height	Width	Height
C2 (axis)	62.5 (43.7)	39.1	37.7[h]	—	—
C3	38.9	42.0	37.8	—	—
C4	38.4	37.4	37.1[h]	—	—
C5	36.7	40.3	34.1	—	—
C6	34.6	40.8	34.1	—	—
C7	36.5	46.4 (55.4)	30.4	—	—
T3?	35.7*	—	33.1	—	—
L3?	51.5	—	40.0	—	—
L4?	51.0	57.7	39.5	—	—
L5?	47.4	56.4	37.8	—	—

section, with broad nasals that extend posteriorly to lap onto a scapanoid or shovel-shaped frontal, with lateral apices formed by narrow supraorbital processes. The orbits themselves are small and located just in front of the lateral apices (arrow in Fig. 12A). The palate is convex on the ventral surface of the skull, as is typical of remingtonocetids, with the space above the palate being filled by narial passages. Roots of a three-rooted P^4 and three-rooted M^1 are preserved, and M^3 is only partially erupted. GSP-UM 1856 (Fig. 12B) includes a rostral fragment with a small single-rooted tooth on each side, probably P^1, with narial passages preserved as stone casts extending forward above this. GSP-UM 3101 is a fragment of a cranium broken on the midline, with part of the orbit, the postorbital process of the supraoccipital, and the frontal sinus exposed. GSP-UM 3101 measures 6.1 cm in breadth across the postorbital process, making the complete skull 12.2 cm in breadth across the postorbital processes (cf. 10.7 cm for GSP-UM 1856 in Table 4; Kumar and Sahni, 1986, p. 333, give this distance as 11.5 cm).

The new specimen of greatest importance is GSP-UM 3057, which includes a good cervical series (Figs. 13A-F, 14) with centra similar to, but smaller than, cervicals associated with specimens of *Dalanistes ahmedi* (see below). This specimen and GSP-UM 3009 include an unusual bone (Fig. 12C) now known, by comparison with a referred skull of *Dalanistes*, to be a remingtonocetid exoccipital. The exoccipital of GSP-UM 3057 is illustrated in Figures 12D and 13K. It has a marked medial waisting that probably explains why exoccipitals are seemingly commonly found broken from the rest of the occiput. The exoccipital has a broad shallowly-concave anterior surface (arrow in Fig. 12C) that contacts the posterior surface of the bulla, and there is a distinctive ventrolateral process (*vlp* in Fig. 12C) with an anterior concavity or depression.

The cervical series of GSP-UM 3057 is illustrated in Figure 13A-F (anterior views) and Figure 14 (lateral views). Three features are worthy of note: (1) all of the cervical centra are long, indicating that the neck as a whole was relatively long for an archaeocete (all of the known cervicals of protocetids are shorter); (2) Ca3 through Ca6 are trapezoidal in lateral profile, indicating that the head was habitually held up above the level of the thorax; and (3) a hypapophysis is well developed on Ca2 through Ca4 and present on Ca5, presumably helping to stabilize the relatively long neck. The hypapophyses on Ca2 and Ca3 are divided (arrows in Figs. 13A,B); the hypapophysis on Ca4 is prominent but undivided; and that on Ca5 is present but neither prominent nor divided. Ca6 and Ca7 lack hypapophyses. Vertebrae com-
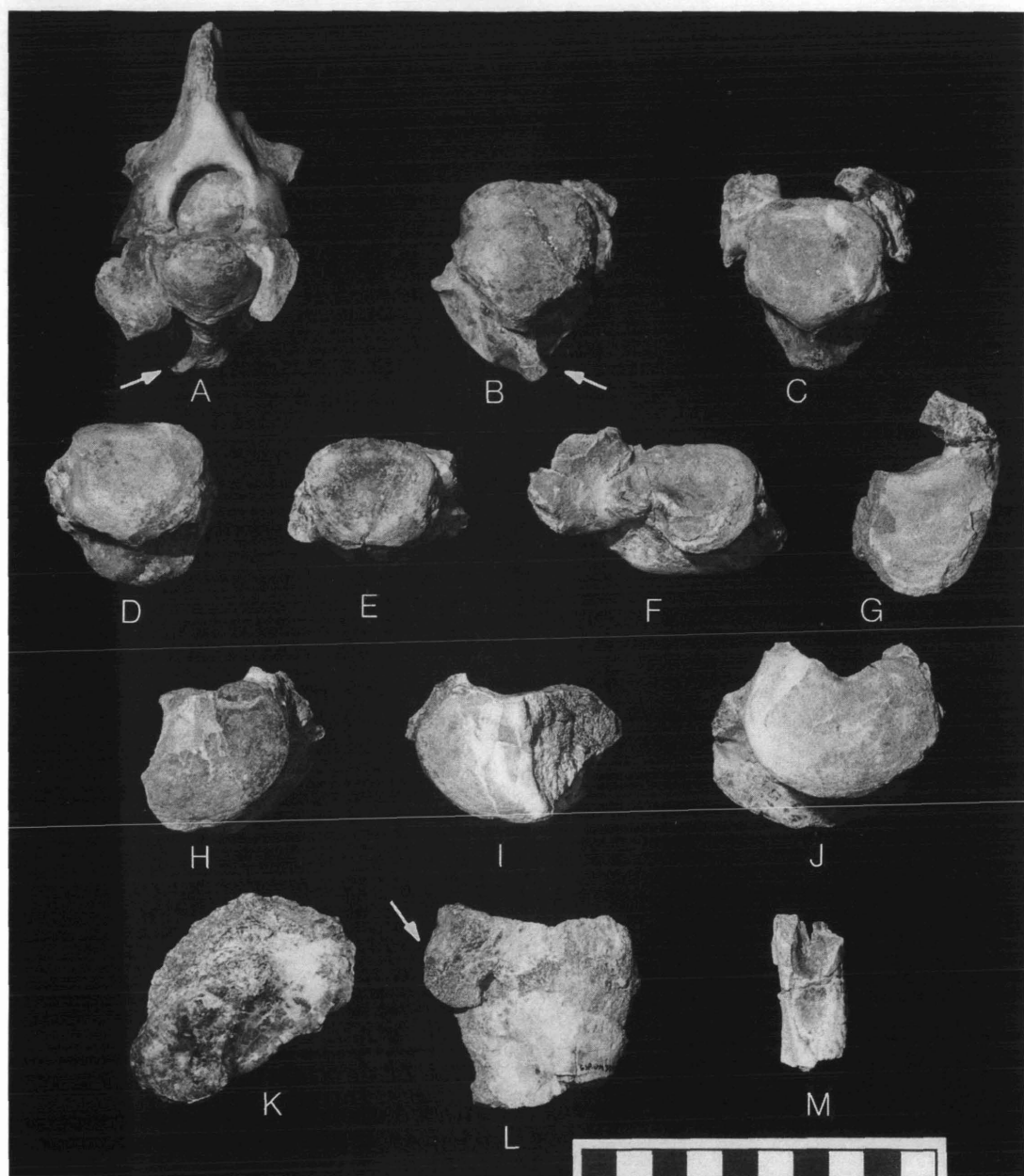
FIG. 13—Cranial and postcranial remains of *Remingtonocetus* cf. *R. harudiensis*, all GSP-UM 3057. A, cervical vertebra C2 (axis). B, centrum of C3. C, centrum of C4. D, centrum of C5. E, centrum C6. F, centrum of C7. G, centrum of thoracic vertebra T3?. H, centrum of lumbar vertebra L3?. I, centrum of L4?. J, centrum of L5?. K, right exoccipital in anterior view. L, fragment of sacrum with parts of centra S1 and S2 fused, in ventral view. M, dentary fragment with alveolus, in dorsal view. Vertebral centra in A-J are all in anterior view. Note large, divided hypophyses on C2 and C3 (arrows), and base of auricular process on S1 (arrow). Scale is in cm.

FIG. 14—Associated cervical vertebrae C2 through C7 of *Remingtonocetus* cf. *R. harudiensis*, all GSP-UM 3057. Vertebrae are shown in right lateral view; anterior is to right. Note lengths and trapezoidal outlines of individual centra, indicating that the neck as a whole was long for an archaeocete and the resting posture of the skull was high compared to the rest of the body. Scale is in cm.

plete enough to show this indicate that Ca3 through Ca6 have foramina lateral to the centrum; these carry a vertebral artery supplying the brain in most mammals. Cervicals of GSP-UM 3009 and 3015 described by Gingerich et al. (1993) are identical to those described here (and can now be identified with certainty to position in the neck).

Partial vertebrae from the thorax and lumbus were found with GSP-UM 3057, but there are not enough of these to enable them to be identified with certainty. This specimen also includes parts of the fused first two centra of a sacrum (S1 and S2; Fig. 13L). A sacrum composed of multiple fused centra (S1-S4) is characteristic of remingtonocetids and the sacrum from the *Remingtonocetus harudiensis*-bearing bed at the type locality, described by Sahni and Mishra (1975) as moeritheriid, almost certainly belongs to this species. No innominates were found with GSP-UM 3057, but that with GSP-UM 3015 (Gingerich et al., 1993, fig. 12B) has a conspicuous depression in the ilium just anterior to the acetabulum. The innominate from the *R. harudiensis*-bearing bed at the type locality described by Sahni and Mishra (1975) as sirenian is similar and almost certainly belongs to this species too. Measurements of vertebrae of *Remingtonocetus* cf. *R. harudiensis* are given in Table 5.

Part of the proximal end of a femur was found in 1992 with GSP-UM 3015 (Gingerich et al., 1993, fig. 13A). In 1994 we found a much more complete femur (GSP-UM 3054, Fig. 15A,B), and an associated proximal tibia (Fig. 15C). These are identified as *Remingtonocetus* because of their size and because they so closely resemble remains of both bones described previously. The new femur has the head well preserved. This is spherical, 3.60 cm in diameter, with a very shallow fovea capitis femoris for insertion of a round ligament. This is in about the same position as it is in a canid, and is more easily located by feel than by sight. The greater trochanter rises high above the femoral head (Fig. 15). There is a smaller lesser trochanter below the head, and a crest connecting the two encloses a deep trochanteric fossa (*tf*) for insertion of obturator muscles extending and rotating the femur. In addition, there is a distinct swelling opposite the second trochanter that indicates the presence of a rudimentary third trochanter. The femoral shaft is unusual in having an oval cross-section, with a conspicuous lateral keel that is concave on its posterolateral surface (arrow in Fig. 15A) for

FIG. 15—Left femur and associated proximal tibia of *Remingtonocetus* cf. *R. harudiensis*, all GSP-UM 3054. Femur, lacking condyles, is shown in posterior (A) and anterior views (B). Proximal tibia is shown in anterior view (C). Specimen is identified as *Remingtonocetus* because femur and tibia are similar to those of GSP-UM 3015 described by Gingerich et al. (1993). Note high greater trochanter (*gt*) rising above the femoral head, and the deep trochanteric fossa (*tf*) for obturator muscles extending and rotating the femur. Femoral shaft is unusual in bearing a conspicuous lateral keel, that is concave posterolaterally (arrow) for insertion of powerful extensors and adductors. One-half natural size; scale is in cm.

insertion of extensor and adductor musculature. The length of the femur cannot be measured because the distal end is missing, but, taking this into account, it appears to have been about 22 cm long with the greater trochanter included and 20 cm long if this is excluded. The midshaft measures 2.44 cm in anteroposterior diameter and 3.44 cm in mediolateral diameter with the lateral keel. Much of the distal end of the femur is missing, including the patellar trochlea on the anterior surface and both condyles on the posterior surface. However, the flaring that remains indicates that the distal end of the femur was broad, and the patellar groove, however wide, was not raised like that of *Rodhocetus*. The new proximal tibia is the size of the proximal tibia described previously (Gingerich et al., 1993, fig. 13B), but is otherwise uninformative. Now that we have a good estimate of femur length in *Remingtonocetus* (22 cm), it is worth recalling that proximal and distal parts of the tibia described previously total 24 cm long and the total length may have been greater (depending on how

much of the midshaft is missing). The tibia was longer than the femur, unlike the condition in *Basilosaurus* (Gingerich et al., 1990).

Discussion.—New specimens collected in 1994 clearly show that the two postcranial skeletons attributed to *Indocetus ramani* by Gingerich et al. (1993), GSP-UM 3009 and 3015, are remingtonocetid rather than protocetid, and thus these cannot be *Indocetus*. GSP-UM 3009 and 3015 are remingtonocetid because they include an exoccipital now known, by comparison with *Dalanistes* (described below), to be remingtonocetid, they have long cervical vertebrae, and they have a sacrum with fused centra. These and other elements are similar to, but smaller than, comparable elements of *Dalanistes*.

From the time it was named by Kumar and Sahni (1986), *Remingtonocetus* has been known to have had an unusually long and narrow skull, with the long rostrum and specializations of the ear suggesting an aquatic habitus. The postcranial skeleton of *Remingtonocetus* now appears to have been as distinctively specialized as the skull, with many features suggesting a terrestrial habitus. The neck is unusually long for an archaeocete, retaining cervical centra longer than those of anterior thoracics, as is typical of land mammals. The sacrum contains four centra, which are solidly fused (Gingerich et al., 1993), the pelvis is large and articulates with the sacrum, and the femur and tibia are substantial, which, taken together, show *Remingtonocetus* to have retained a powerful hind limb capable of bearing the animal's weight on land. *Remingtonocetus*, with features of both aquatic and land mammals, was clearly an amphibious intermediate of some kind. Interpretation of its locomotion and feeding will require better knowledge of the forelimb, hind foot, and tail.

Dalanistes ahmedi, new genus and species
Figs. 17-20

Holotype.—GSP-UM 3106, partially articulated skull and postcranial skeleton.

Type locality.—Basti Ahmed, in Dalana Nala drainage in saddle just to the south of Takra valley, 30°07'33" N latitude, 70°21'55" E longitude (Fig. 16).

Referred specimens.—Pinfold collection: NHML M50719 (cranium, cervical C6). 1981 collection: GSP-UM 11, partial sacrum (S1-S2 described by Gingerich et al., 1993, p. 405). 1994 collection: GSP-UM 3045, lumbar vertebra; 3052, cranium; 3089, innominate; 3096, cervical vertebra (C3); 3097, lumbar vertebra; 3099, partial cranium and associated vertebrae (Ca1?, Ca4?); 3102, sacrum (S1-S4); 3109 (lumbar vertebra); 3115, distal femur.

Age and distribution.—*Dalanistes ahmedi* is known from several localities in the lower and middle parts of the Domanda Formation at the southern end of the Zinda Pir anticlinorium and Rakhi Nala in the Sulaiman Range, Punjab, Pakistan. These are all late early Lutetian (middle Eocene) in age.

Diagnosis.—Similar to *Remingtonocetus harudiensis* and *R. sloani* but differs in being some 20% larger; having external nares open above C^1 rather than P^1; having much higher sagittal and nuchal crests, with the rostrum distinctly angled downward relative to the orientation of the braincase (clinorhynchy); retaining an open mandibular symphysis (synchondrosis) that ends at P_3 rather than P_4; and having mandibular canals in left and right dentaries separate throughout their length. Differs from *Andrewsiphius kutchensis* and *A. minor* in being larger; retaining an open mandibular symphysis (synchondrosis) that ends at P_3 rather than M_3; and having mandibular canals in left and right dentaries separate throughout their length.

Etymology.—Contraction of *Dalana* and *istes* or *anistes*, Gr. (masc.), recalling the Greek name *platanistes* for the extant Indo-Gangetic river dolphin. *Dalanistes* and *Platanista* cannot be closely related, but both have small orbits and small eyes and each has a distinctively long and narrow rostrum. Generic and specific names both refer to the type locality, near Basti Ahmed on the Dalana Nala side of a drainage divide at the southwestern end of Takra Daab.

FIG. 16—Type locality of *Dalanistes ahmedi* in middle Domanda Formation shales. Locality is south-southeast of Basti Ahmed in the saddle shown in Figure 3. Type specimen was found where collector in white shirt is working, where it was exposed in situ by erosion. Sacrum and pelvis were found where Border Military Police guard is sitting. Vertebral centra and other bones that weathered out before the specimen was discovered were found widely scattered in and along the gully in the foreground. Proximal and distal ends of the femur were found on the slope to the right of the backpack. Ridge-top at left is capped by a distinctive thin marker bed of hard limestone that separates the middle from the upper Domanda Formation elsewhere along strike. View here is to the northwest.

Description.—The skull of the type specimen of *Dalanistes ahmedi* is illustrated in Figure 17, which shows a reassembly of casts of individual parts of the skull. The rostrum anterior to P^4 and posterior to P^2 has been filled, spaced so that alveoli for upper teeth conform in position to alveoli for lower teeth. Similarly, connections of left and right squamosals to the rest of the skull have been reconstructed using GSP-UM 3052 for orientation and spacing. Left and right exoccipitals are missing in the type, as are left and right periotics and tympanics. Salient features of the cranium are: (1) its long and narrow but deep rostrum with external nares opening above C^1 (*n* in Fig. 17B); (2) sulci in the posterolateral surfaces of left and right frontal sinuses showing the position of the optic tracts (with the right orbit having been located just in front of the arrow in Fig. 17B)—some 64% of the cranium was in front of the orbit; (3) the sagittal crest (*s* in Fig. 17B) was as high above the braincase as the braincase itself is deep; and (4) the base of the braincase, as marked by the top of the presphenoid, was oriented at a 20° angle to the long axis of the rostrum, as marked by alveoli of the maxillary tooth row. This clinorhynchy is much more strongly developed than is seen in non-remingtonocetids. Salient features of the mandible are: (5) a symphysis (synchondrosis) between left and right dentaries extending back as far as P_3; (6) dentaries that are deep and narrow in the symphyseal region, but relatively shallow and broad posterior to this; and (7) the well-developed mandibular canals within left and right dentaries—these do not cross the symphysis to unite anteriorly.
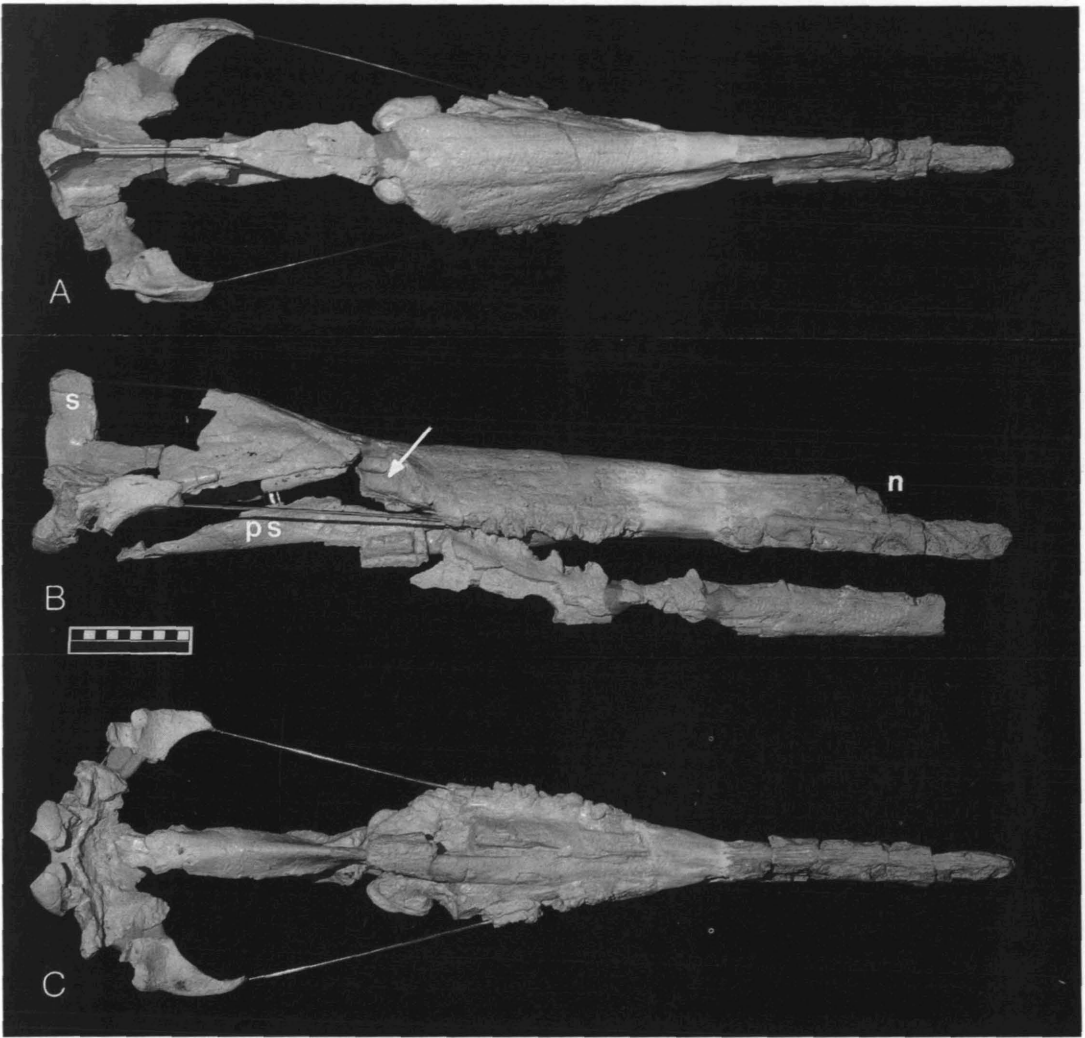
FIG. 17—Reconstructed skull of *Dalanistes ahmedi*, GSP-UM 3106 (holotype), found in the middle part of the Domanda Formation near Basti Ahmed (Fig. 16). A, cranium in dorsal view. B, cranium and part of dentary in right lateral view. C, cranium in palatal view. Anterior is to the right. Clear plexiglass rods stabilize the reconstruction. Note sagittal crest (*s*) rising high above top of braincase, 20° flexure of the neurocranium and splanchnocranium (clinorhynchy), and long, narrow rostrum with external nares opening above C^1 alveolus (*n*). Tip of rostrum with I^1 alveolus is missing due to breakage, and all teeth are missing. Clinorhynchy is here measured in lateral view as the angle formed by the long tooth-bearing part of the maxilla and the base of the brain case overlying the presphenoid (*ps*). A groove (arrow) for the optic tract impressed into the lateral surface of natural stone casts of left and right frontal sinuses shows the position of the orbit on each side of the skull. Scale is in cm.

The dental formula of *Dalanistes* was evidently 3.1.4.3/3.1.4.3, judging from alveoli in the type specimen, although the alveolus for I^1, alveoli for P^3, and alveoli for some lower teeth are not preserved. Measurements of alveoli or roots, when known, are given in Table 6.

TABLE 6—Selected measurements of upper and lower alveoli, diastemata, cranium, and dentary of *Dalanistes ahmedi* based on GSP-UM 3106 (holotype) unless otherwise noted. Abbreviations: D, diastema following tooth; H, height; L, length; W, width. Asterisk marks estimated measurement; superscript *a* indicates estimate is of the length or width of an alveolus (alveoli in the case of teeth with multiple roots).

Cranium

I^1	L:W:H:D:	—	:	—	:	—	:	—	mm
I^2	L:W:H:D (single-rooted alveolus):	18.0^a	:	—	:	—	:	19.1
I^3	L:W:H:D (single-rooted alveolus):	19.3^a	:	—	:	—	:	32.1
C^1	L:W:H:D (single-rooted alveolus):	29.3^a	:	12.4^a	:	—	:	25.4
P^1	L:W:H:D (single-rooted):	27.0^a	:	9.9^a	:	—	:	30.3
P^2	L:W:H:D (double-rooted alveolus):	50.9^a	:	11.8^a	:	—	:	—
P^3	L:W:H:D:	—	:	—	:	—	:	13.4
P^4	L:W:H:D (triple-rooted):	43.5^*	:	18.4^*	:	—	:	—
M^1	L:W:H:D (incipiently triple-rooted):	32.0^*	:	15.3^*	:	—	:	—
M^2	L:W:H:D (double-rooted):	33.9^*	:	14.4^*	:	—	:	—
M^3	L:W:H (double-rooted):	26.0^*	:	11.6^*	:	—	:	—

Skull length (condylobasal):			90.0^*	cm
Diameter of orbit:			—	
Diameter of infraorbital foramen:			--	
Breadth of frontal shield at postorbital process (maximum):			13.0^*	
Breadth across nasals on frontal shield (maximum):			6.7	
Breadth of rostrum at C^1:			3.6	
Breadth of rostrum at P^2:			3.7	
Breadth of palate at M^3:			13.1	
Height of skull above palate at M^{2-3}:			8.8	
Breadth of skull across zygomatic arches (maximum):			26.0^*	
Breadth of skull across squamosals:			24.0	
Breadth of skull across exoccipitals (GSP-UM 3052):			23.0	
Foramen magnum W:H:		4.8 :	2.2	
Height of nuchal crest above foramen magnum (maximum):			12.5	
Tympanic bulla L:W:H (GSP-UM 3052):	7.2 :	4.3 :	4.2	

Mandible

I_1	L:W:H:D:	—	:	—	:	—	:	—	mm
I_2	L:W:H:D:	—	:	—	:	—	:	—
I_3	L:W:H:D:	—	:	—	:	—	:	—
C_1	L:W:H:D (single-rooted alveolus):	23.0^a	:	13.0^a	:	—	:	38.4
P_1	L:W:H:D (single-rooted):	21.2^*	:	9.0^*	:	—	:	26.9
P_2	L:W:H:D (double-rooted alveolus):	44.5^a	:	9.8^a	:	—	:	28.6
P_3	L:W:H:D (double-rooted alveolus):	52.0^a	:	10.5^a	:	—	:	33.4
P_4	L:W:H:D (double-rooted alveolus):	44.3^a	:	12.6^a	:	—	:	—
M_1	L:W:H:D (double-rooted alveolus):	35.9^a	:	14.5^a	:	—	:	—
M_2	L:W:H:D (double-rooted):	32.4^*	:	10.9^*	:	—	:	—
M_3	L:W:H (double-rooted):	29.9^*	:	10.2^*	:	—	:	—

Length of right dentary from front of C_1 alveolus to back of M_3 alveolus:			41.2	cm
Depth of dentary below C_1:			3.2	
Depth of dentary below P_{3-4}:			--	
Depth of dentary below M_1:			—	
Depth of dentary below M_3:			—	
Posterior opening of mandibular canal W:H:		— :	—	
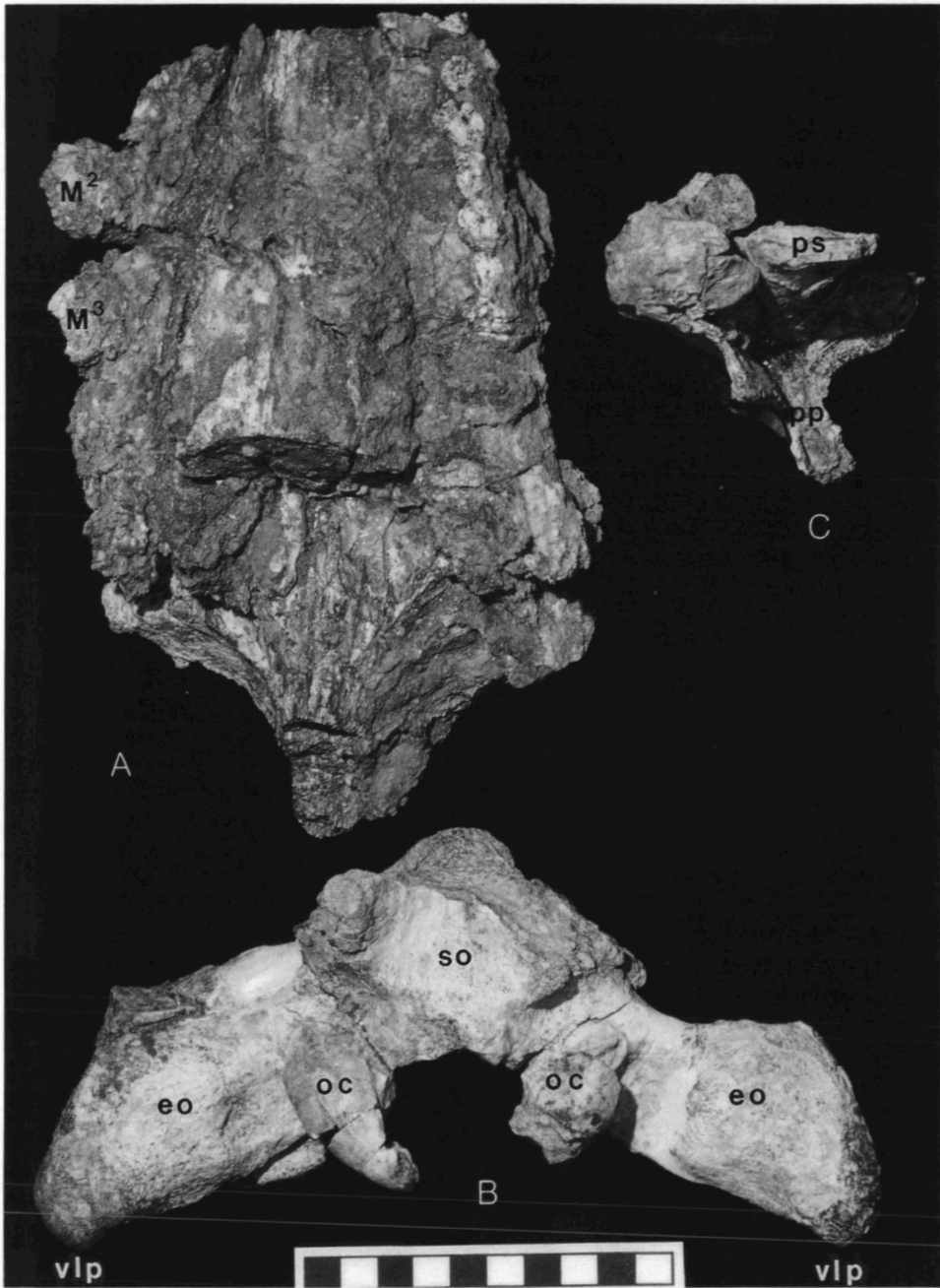
FIG. 18—Parts of referred skull of *Dalanistes ahmedi*, GSP-UM 3052, from the lower part of the Domanda Formation southwest of Takra pond. A, middle part of skull in palatal view with gypsified M$^{2-3}$ preserved on right side of palate and two-rooted alveoli for these teeth preserved on left side (anterior is toward top). B, occiput in posterior view showing supraoccipital (*so*), occipital condyles (*oc*), and distinctive remingtonocetid exoccipitals (*eo*) with ventrolateral processes (*vlp*). C, cross-section of basicranium showing presphenoid (*ps*) and enveloping vomer, and ventrally-directed palatine-pterygoid midline keel (*pp*) enclosing narial passages. Scale is in cm.
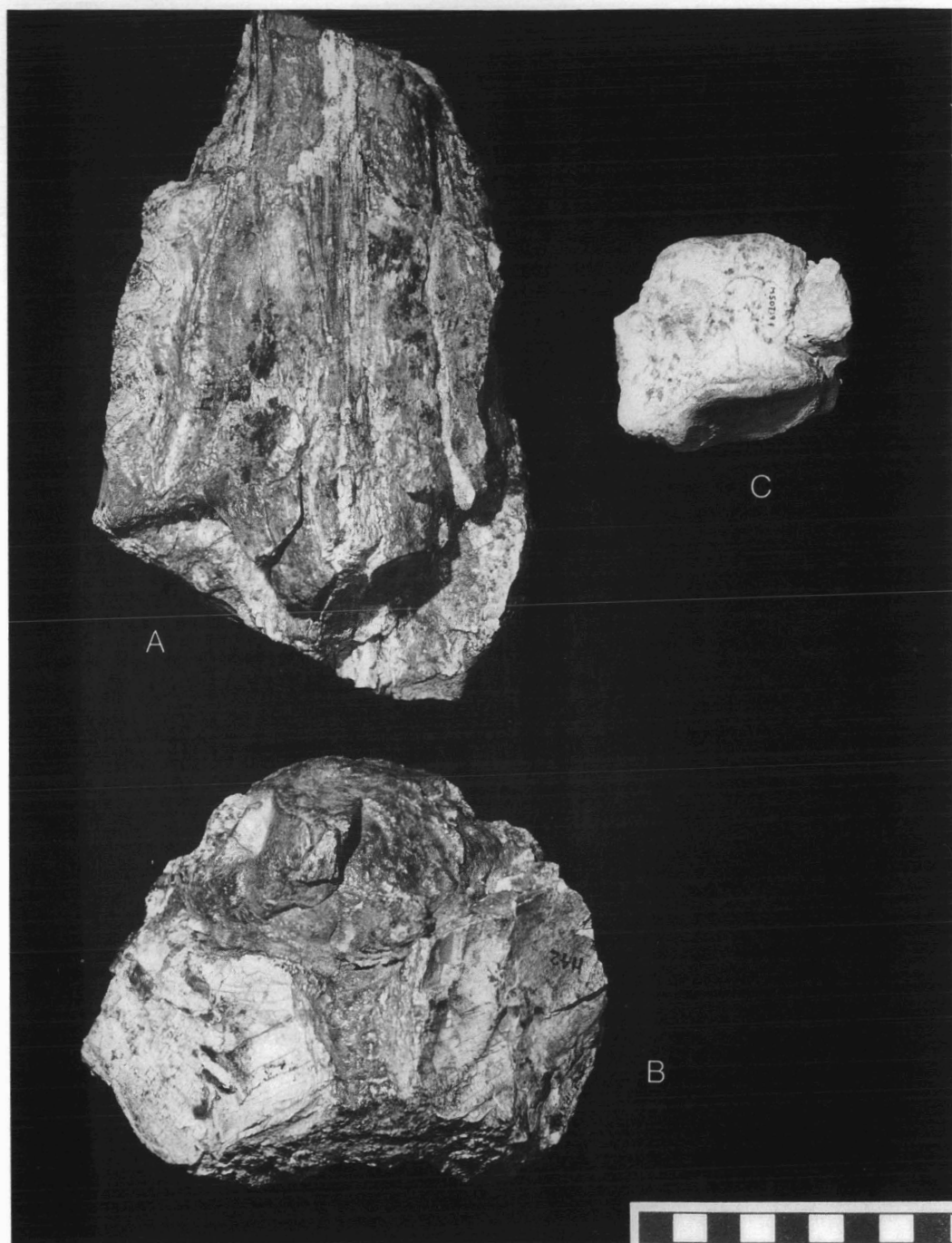
FIG. 19—Parts of referred skull and vertebra of *Dalanistes ahmedi*, NHML M50719, from the lower part of the Domanda Formation in Rakhi Nala. A, middle part of skull with convex palate in palatal view, with roots for double-rooted M^{2-3} preserved on right side (anterior is toward top). B, occiput in dorsal view. C, cervical vertebra C6 in dorsal view. Ribs and relatively short anterior thoracic vertebrae from Pakistan catalogued under this number are preserved differently and are not likely to be part of the same specimen. Scale is in cm.
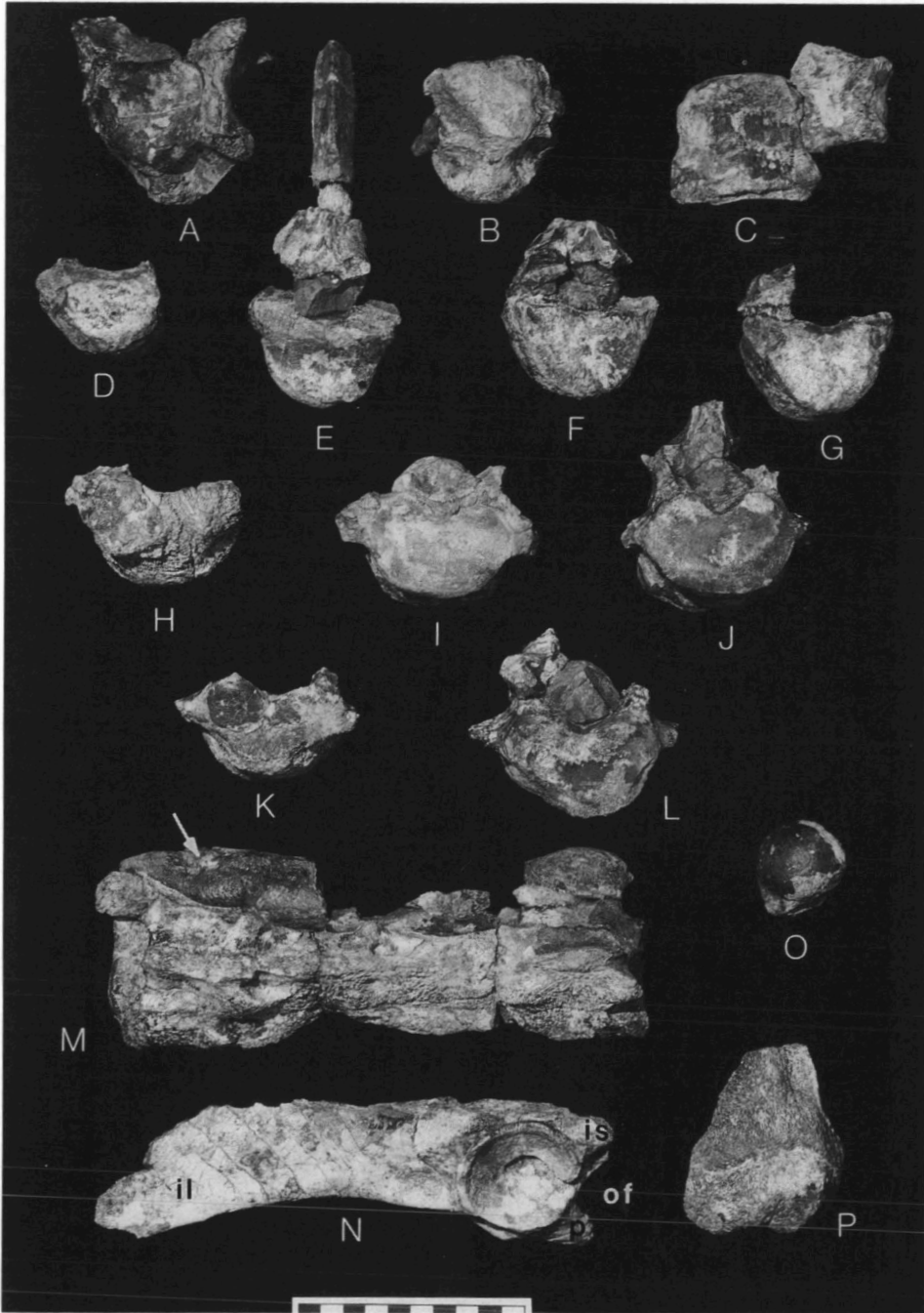
FIG. 20—Vertebrae and hind limb remains of *Dalanistes ahmedi*, GSP-UM 3106 (holotype). A, centrum of C3. B, C5. C, T1. D, T2?. E, T4?. F, T5?. G, T6?. H, L2?. I, L3?. J, L4?. K, L5?. L, L6?. M, sacrum with S1-S4. N, left innominate with massive ilium (*il*), large acetabulum, and ischium (*is*) and pubis (*p*) surrounding obturator foramen (*of*). O, head of femur. P, distal end of femur with shallow patellar groove. Sacrum has centra of S1-S3 solidly co-ossified and S4 was an immovable part of the sacrum. Note auricular process preserved on right side of sacrum (arrow) for articulation with ilium of right pelvic bone. Scale is in cm.

TABLE 7—Sizes of vertebrae of *Dalanistes ahmedi*, based on GSP-UM 3106 (Fig. 20) and 3099 (caudals associated with a cranium). Asterisk marks estimates. Centrum lengths of sacral vertebrae are measured to and/or from centers of sacral foramina; widths and heights of S1 are for anterior face of centrum and anterior opening of neural canal, those for S4 are for posterior face and opening. Total length of sacrum is 236 mm. Measurements are in mm.

Vertebra	Centrum			Neural canal	
	Length	Width	Height	Width	Height
GSP-UM 3106 (holotype)					
C3	55.1	55.7	44.0	16.5*	25.5*
C5	49.3	53.6	46.9	--	--
T1	51.5	66.6	35.5	31.0*	--
T2?	45.9	--	37.2	--	--
T4?	49.6	64.4	43.3	--	--
T5?	49.5	64.1	41.9	--	--
T6?	51.3	67.4	42.4	28.0*	21.0*
L2?	63.2	73.8	49.0	31.1*	24.2*
L3?	60.5	68.7	40.4	--	--
L4?	57.4	68.2	46.3	30.6*	20.6*
L5?	54.4	65.7	45.0	34.2*	22.0*
L6?	54.6	67.4	46.2	--	--
S1	60.5*	64.5	48.0	24.4	15.5
S2	46.4*	--	--	--	--
S3	60.3*	--	--	--	--
S4	63.3*	52.4	42.3	25.5	15.0
GSP-UM 3099					
Ca1?	60.0*	62.5	44.5	20.5	10.0
Ca4?	73.5	55.0*	50.0	17.1	11.8

Unfortunately, without well preserved crowns it is impossible to tell how high-crowned any of the teeth of *Dalanistes* were in life. Upper incisors and the upper canine are represented by alveoli only. These suggest simple teeth with labiolingually-constricted roots (and crowns). The root of P^1 is preserved on the right side in the type, and this is labiolingually-constricted with a suggestion of division of one root into two. Alveoli show P^2 to have been a long and narrow, two-rooted tooth. The section of maxilla that carried P^3 is missing. P^4 has part of the crown preserved, showing that this was a long, narrow tooth, with a distinct protocone root positioned lingually near the back of the tooth. M^1 and M^2 are similar in outline to P^4, but shorter and narrower, with a weaker protocone root (indistinct on M^2). M^3 appears to have been a simple, narrow, double-rooted tooth. There are shallow embrasure pits between C^1 and P^1 and between P^1 and P^2 on the maxilla and very shallow depressions anterolingually to P^4 and the upper molars, but these are not as well developed as those of protocetids, suggesting that cheek teeth of *Dalanistes* were lower-crowned.

The palate of *Dalanistes* is markedly convex ventrally where the maxillae and palatines cover the narial passages. This ventral convexity, plus slight lateral splaying of upper cheek teeth and the smooth curvature of the dorsal surface of the rostrum give remingtonocetids a distinctive transverse cross-section in the middle of the skull.

The orbits are not well preserved in any specimens of *Dalanistes* found to date, but distinct sulci in the posterolateral surfaces of left and right frontal sinuses show where these were located (these frontal sinuses are visible in all three views of the type skull in Fig. 17). The frontal bones rise just posterior to the exposed frontal sinuses, and the dorsal sutures with

parietals lie well in front of the intertemporal constriction.   Frontals in *Dalanistes*, like *Remingtonocetus*, are scapanoid or shovel-shaped, with lateral apices (here broken) formed by narrow supraorbital processes. Posterior to the frontal-parietal suture, parietals rise above the roof of the braincase to form a high sagittal crest.

The floor of the braincase is formed in part by the basisphenoid-presphenoid, which rises conspicuously toward the front of the braincase. Whether this, or the parallel orientation of the olfactory peduncle, is taken as the orientation of the brain, the braincase or neurocranium makes an oblique angle of about 160° to the long axis of the splanchnocranium or facial part of the skull. Stated in other terms, the long axis of the facial part of the skull is depressed by ca. 20° relative to the orientation of the braincase, making it notably clinorhynchous.

The only part of the brain preserved as a natural endocast in the type specimen is the long olfactory peduncle, which measures about 14 × 12 mm in cross-section. The inside of the braincase is raised in the midline anterodorsally, indicating the presence of a substantial dorsal sagittal sinus. This is followed posteriorly by a conspicuous tentorial protuberance in the dorsal midline of the braincase (indicating the presence of a tentorial fossa in the dorsal surface of the brain itself).   This tentorial fossa divides the cerebrum anteriorly from the cerebellum posteriorly. The skull roof, as preserved, indicates that the cerebrum had a smooth dorsal surface. The dorsal surface of the cerebellum was less smooth, but *Dalanistes* clearly lacked the massive rete mirabile found lying on top of the cerebellum in basilosaurid archaeocetes. GSP-UM 3052 (Fig. 18) and NHML M50719 (Fig. 19) preserve substantial parts of the brain in the form of natural stone endocasts, but these have not yet been prepared for study.

Large parts of the basicranium, including the basisphenoid, both periotics, and both auditory bullae, are missing in the type of *Dalanistes*. Squamosals on the left and right sides preserve the glenoid fossae for articulation with the dentaries, postglenoid processes, and external auditory meatae.   Occipital condyles are massive, and the supraoccipital is deeply concave above the foramen magnum.

Referred specimen GSP-UM 3052 (Fig. 18) includes the middle part of a skull with roots for double-rooted M^2 and M^3 located on the convex palate well forward of the zygomatic arch. It also includes the posterior part of the skull showing the broad exoccipitals (*eo* in Fig. 18B) that flank the occipital condyles, sloping downward to conspicuous ventrolateral processes (*vlp*). This specimen preserves the left tympanic bulla in place in front of the exoccipital (not visible in Fig. 18B). The bulla is similar to that of *Gaviacetus* described above in having a lateral surface that is flat and nearly circular, but the plane of the surface converges anteriorly toward the midline rather than being parasagittal. The sigmoid process develops from the middle of the circular lateral surface rather than its anterior edge. As in *Gaviacetus*, a narrow sulcus separates the flat lateral surface of the lateral lobe of the bulla from an ovally-involuted anterior lobe, and a broader shallow sulcus separates both from an ovally-involuted posterior lobe.

It is difficult to give a full characterization of articulation of the auditory bulla with the rest of the skull because the bulla is in place in the only specimen preserving this region of the skull.   It is not clear, for example, whether the anterior lobe of the bulla has a dorsal synchondrosis with a broad, flat, circular surface of the squamosal like that in *Gaviacetus* and other protocetids. The posterior process of the lateral lobe of the bulla does appear to have a dorsal synostosis with the posterior process of the periotic. The most distinctive connection of the bulla to the rest of the skull is a broad connection of the posterior lobe of the bulla with a flat paroccipital surface (rather than a narrow process) of the exoccipital in another synchondrosis. In addition, the sigmoid process of the lateral lobe lies close to if not actually in a groove in the squamosal, and there is definitely a contact between the medial surface of the posterior lobe of the bulla and the exoccipital part of the falcate process just anterior to the jugular notch.

Finally, referred specimen GSP-UM 3052 is notable in having pterygoids flooring the narial passages beneath the presphenoid drawn downward into a distinctive midline pterygoid process

(*pp* in Fig. 18C), presumably for attachment of pterygoid masticatory muscles manipulating the dentaries.

The type specimen, GSP-UM 3106, includes associated cervical, thoracic, and lumbar vertebrae (Fig. 20A-L). Cervicals are larger but otherwise identical to comparable elements in *Remingtonocetus* described above. Thoracics are similar also, with one including much of a high neural spine (Fig. 20E). Lumbars are large and relatively flat. It is not be possible at this point to confidently identify individual thoracic and lumbar vertebrae. Measurements of vertebrae are listed in Table 7.

The most interesting postcranial elements of *Dalanistes* found to date are pelvic and hind limb elements associated with the type specimen. These include a nearly complete sacrum (Fig. 20M), with four vertebral centra solidly joined to make a massive base for attachment of hind limbs and hind limb musculature. The total length of this sacrum is 236 mm. There is a well developed auricular surface on the sacrum (arrow in Fig. 20M) for articulation with the ilium of the pelvis. A second sacrum, GSP-UM 3102, is even larger, measuring 251 mm in total length.

The ilium itself is robust and long; the ramus measures 4.5 cm deep where it narrows anterior to the acetabulum. The acetabulum is large, measuring 4.75 cm in diameter, with a raised lunate surface and distinct acetabular fossa opening posteroventrally beneath an acetabular notch like that of *Remingtonocetus*. The acetabular notch angles upward behind the lunate surface where it is 1.65 cm deep. The ischium is 2.85 cm deep where it is broken distally, and the pubis is 2.05 cm deep where it is broken; these originally enclosed a large obturator foramen. There is a distinct depression for muscle attachment in the shape of an isoceles right triangle on the lateral surface of the ilium just anterior to the acetabulum; the two equal sides of the depression measure about 2.5 cm.

The head and distal end of a right femur were found close to each other when GSP-UM 3106 was collected. The femoral head is spherical, 4.10 cm in diameter, but incomplete and the position of the fovea capitis femoris could not be located. The distal end of the type femur is broad, with a shallow patellar groove on the anterior surface and low condyles on the posterior surface. The medial condyle appears to have been substantially larger than the lateral condyle. GSP-UM 3115 is an isolated distal right femur that is identical to that in the type, but a little better preserved. It shows that the patellar groove is angled outward distally relative to the long axis of the shaft. Taken together, the sacrum, innominate, and femur indicate the presence of a substantial hind limb in *Dalanistes*.

No caudal vertebrae were found associated with the type specimen, but GSP-UM 3099 is a partial cranium of *Dalanistes ahmedi* with associated well-preserved caudals interpreted as Ca1 and Ca4 (measurements in Table 7). The first has a well preserved neural arch, with a relatively large neural canal for a caudal, and it has truncated, backwardly directed transverse processes with broad ends that undoubtedly fit between ischia of the pelvis in life. It is larger, but otherwise similar to the anterior caudal of *Remingtonocetus* illustrated in Gingerich et al. (1993, figs. 7D and 8D). The second is interpreted as Ca4, although this is not known with certainty. It too has a relatively large neural canal for a caudal, indicating that it belongs somewhere near the anterior end of the tail. The neural arch with its pre- and postzygapophyses is positioned well forward on the centrum and it is doubtful that the postzygapophyses could have contacted prezygapophyses of the following vertebra. There are two transverse processes on each side of the centrum, divided by a circular notch that has the appearance of a foramen. However, closer inspection shows that the anterior processes are complete or nearly so, and there was no arch of bone closing a lateral foramen. Without the neural arch, this caudal is similar to H-GSP 18472, an anterior caudal of *Ambulocetus natans* illustrated by Thewissen et al. (1994, fig. 1B).

Discussion.—Dalanistes is similar in many ways to *Remingtonocetus*, and there is little doubt that they are closely related. However, the position of the external nares, conformation and orientation of the braincase, and fusion of the dentaries distinguish the two genera. There are

TABLE 8—Differences distinguishing skulls and postcranial skeletons of middle Eocene Protocetidae and Remingtonocetidae.

	Protocetidae	Remingtonocetidae
1.	Length of cranium approximately 3× breadth across frontals	Length of cranium approximately 6× breadth across frontals
2.	Preorbital rostrum less than 60% of total skull length	Preorbital rostrum more than 60% of total skull length
3.	Orbits medium to large in diameter relative to rest of skull	Orbits small relative to rest of skull
4.	Nares open above C^1, P^1, or P^2	Nares open above C^1 or P^1
5.	Frontals sphyroid or hammer-shaped	Frontals scapanoid or shovel-shaped
6.	Incisors and premolars circular in cross-section and robust	Incisors and premolars narrow labiolingually
7.	Upper molars generally small and broad, with two lateral roots and a distinct medial root	Upper molars generally larger and narrow, sometimes double-rooted and lacking medial root
8.	Palate flat or concave ventrally	Palate convex ventrally
9.	Bulla articulation with rest of skull includes a narrow paroccipital synchondrosis	Bulla articulation with rest of skull includes a broad paroccipital synchondrosis
10.	Exoccipitals rectangular, robustly integrated with squamosal, and solidly attached to rest of skull	Exoccipitals tapering downward, loosely attached to squamosal, and separated from basioccipital by a waisted section that often breaks
11.	Cervical centra are shorter than they are wide or high, and shorter than anterior thoracic centra	Cervical centra are as long as they are wide or high, and as long or longer than anterior thoracic centra
12.	Sacrum is composed of four or fewer vertebral centra, with sacral centra generally not fused to each other	Sacrum is composed of four vertebral centra, with centra of S1-S3 and generally S4 solidly fused to each other
13.	Innominate with smooth lateral surface in front of acetabulum, with a shallow acetabular fossa and no distinct acetabular notch	Innominate with distinct depression on lateral surface in front of acetabulum, with a deep acetabular fossa and a distinct acetabular notch
14.	Femoral head with distinct, deep fovea for round ligament	Femoral head with shallow or indistinct fovea for round ligament
15.	Femoral shaft round; distal femur narrow relative to shaft diameter, with a narrow, raised patellar groove	Femoral shaft oval in cross-section, with lateral keel for muscle insertion; distal femur broad relative to shaft diameter, with a broad, shallow patellar groove

similarities to *Ambulocetus natans* (Thewissen et al., 1994), described as a protocetid, particularly in the size of the hind limb, but the hind limbs differ in detail when homologous elements like the distal femur are compared (the distal femur of *Dalanistes* has a higher, narrower patellar trochlea, and larger, more posteriorly-deflected condyles).

Dalanistes, like *Remingtonocetus* discussed above, combines features of both aquatic and terrestrial animals, and it was clearly an amphibious intermediate of some kind, but interpretation of its locomotion and feeding will require better knowledge of the forelimb, hind foot, and tail.

COMPARISON OF PROTOCETIDAE AND REMINGTONOCETIDAE

New Protocetidae described here are important in showing that the family included a range of trophic specializations early in its diversification. *Protocetus atavus* is similar in rostral

proportions to later basilosaurids in having a rostrum of medium width. *Indocetus ramani* and *Rodhocetus kasrani* are similar in size and rostral proportions to *Protocetus*, and thus it seemed reasonable to assume that this general form is a stereotypical pattern characteristic of all early protocetids. However, *Takracetus simus* described here shows that at least one early protocetid had a broad and relatively flat rostrum, and *Gaviacetus razai* described here shows that at least one other early protocetid had a narrow rostrum. Thus it is no longer certain what to expect as the primitive condition.

Remingtonocetidae described here are important in untangling previous confusion in the identification of protocetid and remingtonocetid cranial and postcranial remains. While relatively complete skulls of protocetids and remingtonocetids known previously could not be confused (Kumar and Sahni, 1986), it was not clear how different these are in details of the skull nor how different these are in postcranial morphology. Fifteen differences distinguishing skulls and postcranial skeletons of middle Eocene Protocetidae and Remingtonocetidae are listed in Table 8. The first eight of these characteristics were generally known before (Sahni and Mishra, 1975; Kumar and Sahni, 1986). New specimens show that the relationship of the bulla to the paroccipital process or surface of the exoccipital is different in the two families, and the shape and integrity of the exoccipital itself is very different.

Postcranial remains attributed to *Indocetus* by Gingerich et al. (1993) are here assigned to *Remingtonocetus* because they are now known to include associated exoccipitals of remingtonocetid type, and because they are similar to postcranial remains of the new remingtonocetid *Dalanistes*. Remingtonocetids retain longer cervical vertebrae and hence longer necks, and they retain synostosed sacral vertebrae forming a large stiff sacrum for attachment of a large hind limb. This greatly limits their potential for tail-powered swimming, because they cannot be sufficiently caudalized to swim in the manner of modern cetaceans. Three protocetids, *Rodhocetus*, *Takracetus*, and *Protocetus*, are now known to have lost fusion of sacral vertebrae, reflecting their greater caudalization and the development of tail-powered swimming like that of modern cetaceans. Of the two families of archaeocetes known at the end of the early Lutetian, Protocetidae are much more like later Basilosauridae and later modern whales, and Protocetidae are much more likely than Remingtonocetidae to be ancestral to later Basilosauridae and later modern Cetacea.

ACKNOWLEDGMENTS

LITERATURE CITED

BHATTI, M. A., R. AHMAD, S. H. HUSSAIN, and S. JAVED. 1988. Geology of the Choti Bala area, Dera Ghazi Khan and Rajanpur districts, Punjab, Pakistan. Geological Survey of Pakistan Information Release, 335: 1-30.

EAMES, F. E. 1951. A contribution to the study of the Eocene in western Pakistan and western India. B. The description of the Lamellibranchia from standard sections in the Rakhi Nala and Zinda Pir areas of the western Punjab and in the Kohat District. Philosophical Transactions of the Royal Society of London, Series B, 235: 311-482.

————. 1952a. A contribution to the study of the Eocene in western Pakistan and western India. C. The description of the Scaphopoda and Gastropoda from standard sections in the Rakhi Nala and Zinda Pir areas of the western Punjab and in the Kohat District. Philosophical Transactions of the Royal Society of London, Series B, 236: 1-168.

————. 1952b. A contribution to the study of the Eocene in western Pakistan and western India: A. The geology of standard sections in the western Punjab and in the Kohat District. Quarterly Journal of the Geological Society of London, 107: 159-171.

————. 1952c. A contribution to the study of the Eocene in western Pakistan and western India: D. Discussion of the faunas of certain standard sections, and their bearing on the classification and correlation of the Eocene in western Pakistan and western India. Quarterly Journal of the Geological Society of London, 107: 173-196.

FRAAS, E. 1904. Neue Zeuglodonten aus dem unteren Mitteleocän vom Mokattam bei Cairo. Geologische und Paläontologische Abhandlungen, Jena, Neue Folge, 6: 197-220.

GINGERICH, P. D. 1977. A small collection of fossil vertebrates from the middle Eocene Kuldana and Kohat formations of Punjab (Pakistan). Contributions from the Museum of Paleontology, University of Michigan, 24: 190-203.

————, M. ARIF, M. A. BHATTI, H. A. RAZA, S. M. RAZA. 1995. *Protosiren* and *Babiacetus* (Mammalia, Sirenia and Cetacea) from the middle Eocene Drazinda Formation, Sulaiman Range, Punjab (Pakistan). Contributions from the Museum of Paleontology, University of Michigan, 29: in press.

————, S. M. RAZA, M. ARIF, M. ANWAR, and X. ZHOU. 1993. Partial skeletons of *Indocetus ramani* (Mammalia, Cetacea) from the lower middle Eocene Domanda Shale in the Sulaiman Range of Pakistan. Contributions from the Museum of Paleontology, University of Michigan, 28: 393-416.

————, S. M. RAZA, M. ARIF, M. ANWAR, and X. ZHOU. 1994. New whale from the Eocene of Pakistan and the origin of cetacean swimming. Nature, 368: 844-847.

————, and D. E. RUSSELL. 1981. *Pakicetus inachus*, a new archaeocete (Mammalia, Cetacea) from the early-middle Eocene Kuldana Formation of Kohat (Pakistan). Contributions from the Museum of Paleontology, University of Michigan, 25: 235-246.

————, D. E. RUSSELL, D. SIGOGNEAU-RUSSELL, J. L. HARTENBERGER, S. M. I. SHAH, M. HASSAN, K. D. ROSE, and R. H. ARDREY. 1979. Reconnaissance survey and vertebrate paleontology of some Paleocene and Eocene formations in Pakistan. Contributions from the Museum of Paleontology, University of Michigan, 25: 105-116.

————, B. H. SMITH, and E. L. SIMONS. 1990. Hind limbs of Eocene Basilosaurus: evidence of feet in whales. Science, 249: 154-157.

————, N. A. WELLS, D. E. RUSSELL, and S. M. I. SHAH. 1983. Origin of whales in epicontinental remnant seas: new evidence from the early Eocene of Pakistan. Science, 220: 403-406.

HAQ, B. U. 1972. Paleogene calcareous nannoflora. I. The Paleocene of west-central Persia and the upper Paleocene-Eocene of West Pakistan. Stockholm Contributions in Geology, 25: 1-56.

————, J. HARDENBOL, and P. R. VAIL. 1987. Chronology of fluctuating sea levels since the Triassic. Science, 235: 1156-1167.

HEMPHILL, W. R., and A. H. KIDWAI. 1973. Stratigraphy of the Bannu and Dera Ismail Khan areas, Pakistan. Geological Survey of Pakistan, Professional Papers, 716-B: 1-36.

IQBAL, M. W. A. 1969. The Tertiary pelecypod and gastropod fauna from Drug, Zindapir, Vidor (District D. G. Khan), Jhalar and Chharat (District. Memoirs of The Geological Survey of Pakistan, 6: 1-94.

KELLOGG, A. R. 1936. A review of the Archaeoceti. Carnegie Institution of Washington Publications, 482: 1-366.

KÖTHE, A., A. M. KHAN, and M. ASHRAF. 1988. Biostratigraphy of the Surghar Range, Salt Range, Sulaiman Range and the Kohat area, Pakistan, according to Jurassic through Paleogene calcareous nannofossils and Paleogene dinoflagellates. Geologisches Jahrbuch, Hannover, Reihe B, 71: 1-87.

KUMAR, K., and A. SAHNI. 1986. *Remingtonocetus harudiensis*, new combination, a middle Eocene archaeocete (Mammalia, Cetacea) from western Kutch, India. Journal of Vertebrate Paleontology, 6: 326-349.

PILGRIM, G. E. 1940. Middle Eocene mammals from north-west Pakistan. Proceedings of the Zoological Society of London, Series B, 110: 127-152.

SAHNI, A., and V. P. MISHRA. 1972. A new species of *Protocetus* (Cetacea) from the middle Eocene of Kutch, western India. Palaeontology, 15: 490-495.

——— and ———. 1975. Lower Tertiary vertebrates from western India. Monograph of the Paleontological Society of India, 3: 1-48.

SAMANTA, B. K. 1972. Planktonic foraminiferal biostratigraphy of the early Tertiary of the Rakhi Nala section, Sulaiman Range, West Pakistan. Journal of the Geological Society of India, 13: 317-328.

———. 1973. Planktonic foraminifera from the Paleocene-Eocene succession in the Rakhi Nala, Sulaiman Range, Pakistan. Bulletin of the British Museum (Natural History), Geology, 22: 421-482.

SATSANGI, P. P., and P. K. MUKHOPADHYAY. 1975. New marine Eocene vertebrates from Kutch. Journal of the Geological Society of India, 16: 84-86.

SHAH, S. M. I. 1991. Lithostratigraphic units of the Sulaiman and Kirthar Provinces, lower Indus Basin, Pakistan. Geological Survey of Pakistan Information Release, 519: 1-82.

SIDDIQUI, Q. A. 1971. Early Tertiary Ostracoda of the family Trachyleberididae from West Pakistan. Bulletin of the British Museum (Natural History), Geology Supplement 9, pp. 1-98.

STROMER, E. 1908. Die Archaeoceti des ägyptischen Eozäns. Beiträge zur Paläontologie und Geologie Österreich-Ungarns und des Orients, Vienna, 21: 106-178.

TANDON, K. K. 1971. On the discovery of mammalian and reptilian remains from the middle Eocene rocks of S.W. Kutch, India. Current Science, 40: 436-437.

———. 1976. Biostratigraphic classification of the middle Eocene rocks of a part of southwestern Kutch, India. Journal of the Palaeontological Society of India, 19: 71-88.

THEWISSEN, J. G. M., S. T. HUSSAIN, and M. ARIF. 1994. Fossil evidence for the origin of aquatic locomotion in archaeocete whales. Science, 263: 210-212.

TRIVEDY, A. N., and P. P. SATSANGI. 1984. A new archaeocete (whale) from the Eocene of India. *In*: N. A. Bogdanov (ed.), Abstracts of 27th International Geological Congress, Moscow, 1: 322-323.

WELLS, N. A. 1984. Marine and continental sedimentation in the early Cenozoic Kohat Basin and adjacent northwestern Indo- Pakistan. Ph. D. Dissertation, University of Michigan, 1-465.

WEST, R. M. 1980. Middle Eocene large mammal assemblage with Tethyan affinities, Ganda Kas region, Pakistan. Journal of Paleontology, 54: 508-533.